

Chapter 2

Coulomb Collisions

The characteristics and effects of Coulomb collisions between charged particles in a plasma are very different from those of the more commonly understood collisions of neutral particles. The fundamental differences can be illustrated by examining trajectories of neutral and charged particles as they move through a partially ionized gas. As shown in Fig. 2.1, neutral particles move along straight-line trajectories between distinct collision events. Collisions occur when neutral atoms or molecules come within about an atomic radius (of order $1 \text{ \AA} = 10^{-10} \text{ m}$ — see Section A.7) of another particle (a neutral or a charged particle) and the electric field force associated with the atomic potential (of order eV) is operative; the resultant “strong,” typically inelastic, collision causes the initial neutral to be scattered in an approximately random direction.

In contrast, as a charged “test” particle moves through an ionized gas it simultaneously experiences the weak Coulomb electric field forces surrounding all the nearby charged particles, and its direction of motion is deflected as it passes by each of them, with the closest encounters producing the largest deflections — see Fig. 2.2. As was discussed in Section 1.1, the Coulomb potential (and hence electric field) around any particular background charged particle in a plasma is collectively shielded out at distances beyond a Debye length. Thus, the only background particles that exert a significant force on the test particle’s motion are those within about a Debye length of its trajectory. However, since plasmas usually have a very large number of particles within a Debye sphere $[(4\pi/3)n\lambda_D^3 \gg 1]$, even in traversing only a Debye length the test particle’s motion is influenced by a very large number of background particles. The Coulomb electric field forces produced by individual background particles are small and can be assumed to be experienced randomly by the test particle as it passes close to individual background particles — as indicated in the electron trajectory shown in Fig. 2.2. The effect of many successive, elastic Coulomb “collisions” of a test particle with background charged particles leads to a random walk (Brownian motion) process. Thus, the effects of the many cumulative small-angle, elastic Coulomb collisions are diffusion of the test particle’s direction of motion (at constant energy in the center-of-momentum frame)

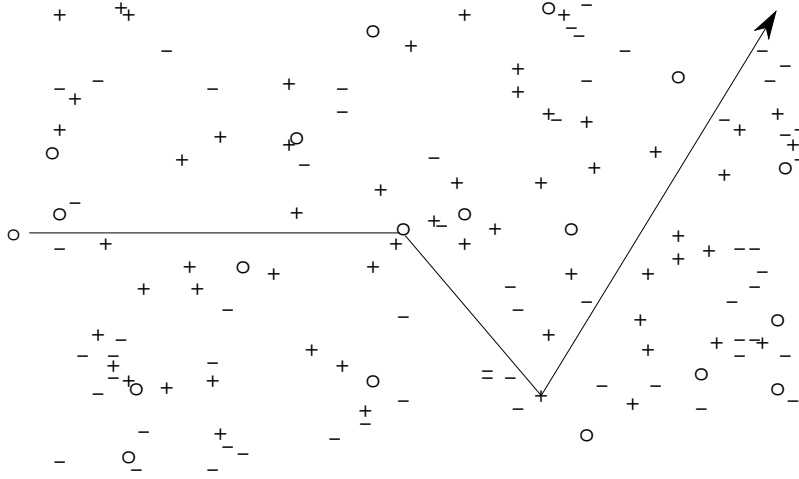


Figure 2.1: The trajectory of a neutral particle in a partially ionized gas exhibits “straight-line” motion between abrupt atomic collisions. In this and the next figure, the (assumed stationary) random positions of “background” particles in the partially ionized plasma are indicated as follows: neutral particles (circles), electrons (minus signs) and ions (plus signs). The typical distance between neutral particle collisions is called the “collision mean free path.”

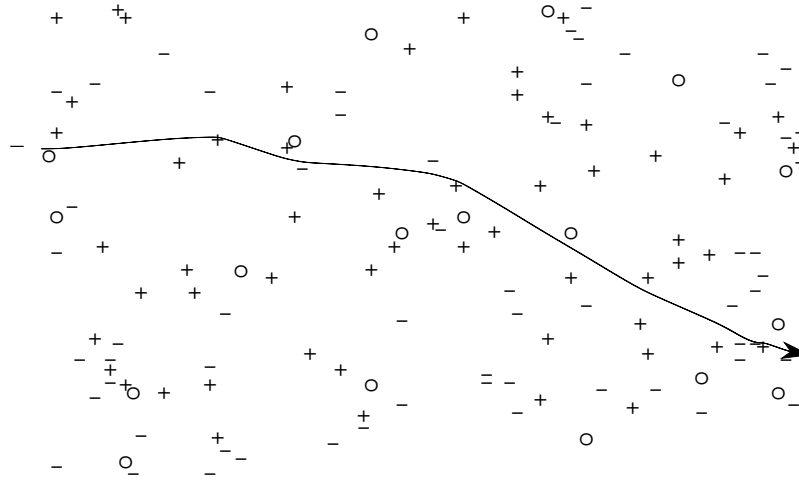


Figure 2.2: The trajectory of a “test” charged particle (electron) in a partially ionized gas exhibits continuous small-angle deflections or scatterings of its direction of motion. The largest deflections occur when it passes close to another charged particle. The “collision length” of a charged particle in a plasma is defined to be the average distance it moves in being deflected through one radian.

and consequently deceleration of the test particle's initial, directed velocity. Exploration of these Coulomb collision effects is the main subject of this chapter.

Because electrons have less inertia and typically have larger speeds than ions, their collision rates are usually the largest in plasmas. Thus, we first consider the momentum loss and velocity-space diffusion of a test electron as it moves through a plasma. Electron collisions are initially investigated using the Lorentz (simplest) collision model in which their collisions are assumed to occur only with a background of stationary ions. Next, since the collisional effects decrease as electron speed increases, we determine the energy (usually on the high energy tail of a Maxwellian distribution) at which electrons “run away” in response to an electric field; also, the plasma electrical resistivity is determined by balancing the average collisional deceleration of an entire flowing electron species against the electron acceleration induced by an electric field. Then, we discuss the various Coulomb collisional processes (momentum loss, velocity space diffusion and energy exchange, and their time scales) that occur between electrons and ions in a plasma. The chapter concludes with sections that develop a more complete model of Coulomb collision effects, both on test particles and on an entire plasma species, that takes into account collisions with all types of background charged particles that are also in motion. Finally, applications of this more complete model to the evolution of the velocity of any type of test particle and to the thermalization of a fast ion in a plasma are discussed.

2.1 Lorentz Collision Model

To illustrate Coulomb collision effects, we first consider the momentum loss and velocity diffusion of a *test* electron moving through a randomly distributed *background* of plasma ions that have charge $Z_i e$ and are stationary. (The particles in the background that are being collided with are sometimes called *field particles*.) The background plasma electrons, which must be present for quasineutrality, will be neglected except insofar as they provide Debye shielding of the Coulomb potentials around the background ions. However, the “test” electron can be thought of as being just one particular electron in the plasma. This simplest and most fundamental model of collisional processes in a plasma is called the *Lorentz collision model*. It provides a reasonably accurate description of electron-ion collisional processes and, in the limit $Z_i \gg 1$ where electron-electron collisional effects become negligible (see Table 2.1 in Section 2.9), for electron Coulomb collision processes as a whole.

The electron test particle velocity \mathbf{v} will be assumed to be large compared to the change $\Delta\mathbf{v}$ due to any individual Coulomb interaction with an ion. Hence, the test electron will be only slightly deflected from its straight-line trajectory during a single collision. Figure 2.3 shows a convenient geometry for describing the Coulomb collision process.¹ In the rest frame of the electron, the background

¹The geometry shown in Fig. 2.3 and the pedagogical approach we use for exploring Coulomb collision processes follows that developed in Chapter 13 of Jackson, *Classical Electrodynamics*, 1st and 2nd Editions (1962, 1975).

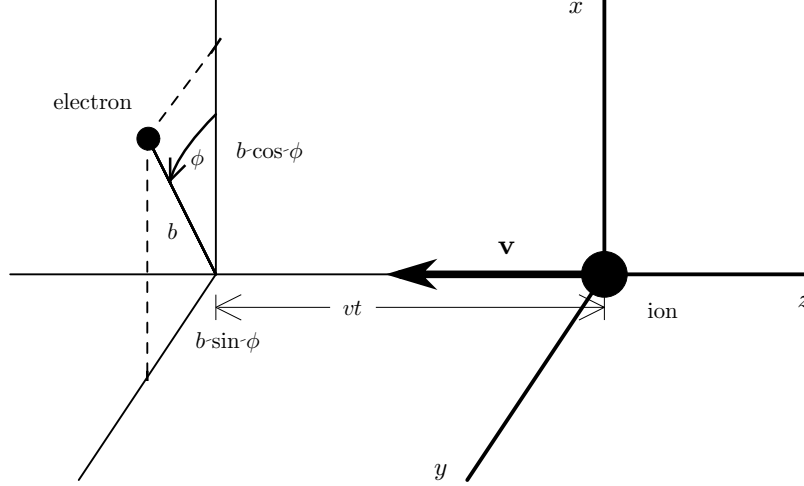


Figure 2.3: Geometry for considering the Coulomb collision of an electron having charge $q_e = -e$ with an ion of charge $q_i = Z_i e$. The ion is placed at the origin of the coordinate system, which in the electron rest frame is moving in the $-\hat{\mathbf{e}}_z$ direction at the electron speed v . The electron passes the ion at an “impact parameter” distance b at the closest point, which occurs at $t = 0$.

ion, which we place at the origin of the coordinate system, is seen to be moving with a velocity $-v \hat{\mathbf{e}}_z$ along a straight-line trajectory $\mathbf{x}(t) = -vt \hat{\mathbf{e}}_z$. The electron is instantaneously at the position

$$\mathbf{x} = b(\hat{\mathbf{e}}_x \cos \varphi + \hat{\mathbf{e}}_y \sin \varphi) + vt \hat{\mathbf{e}}_z, \quad |\mathbf{x}| = (b^2 + v^2 t^2)^{1/2}, \quad (2.1)$$

in which b is known as the *impact parameter*. It is the distance of closest approach, which by assumption will occur at time $t = 0$. The electrostatic potential around the ion is the Coulomb potential $\phi(\mathbf{x}) = Z_i e / (\{4\pi\epsilon_0\} |\mathbf{x}|)$. Thus, the electric field force experienced by the test electron with charge $q_e = -e$ at its position \mathbf{x} is

$$\mathbf{F} = q_e \mathbf{E} = -(-e) \nabla \left(\frac{Z_i e}{\{4\pi\epsilon_0\} |\mathbf{x}|} \right) = - \frac{Z_i e^2 \mathbf{x}}{\{4\pi\epsilon_0\} |\mathbf{x}|^3}. \quad (2.2)$$

Next, we calculate the momentum impulse $m_e \Delta \mathbf{v}$ on the test electron as it passes the background ion. Integrating Newton’s second law ($m d\mathbf{v}/dt = \mathbf{F}$) over time from long before ($t \rightarrow -\infty$) to long after ($t \rightarrow +\infty$) the Coulomb “collision” that takes place during the time t where $|t| \sim \Delta t \sim b/v$, we see that

a single electron-ion Coulomb collision induces:

$$m_e \Delta \mathbf{v} = \int_{-\infty}^{\infty} dt q_e \mathbf{E} = - \int_{-\infty}^{\infty} dt \frac{Z_i e^2 \mathbf{x}}{\{4\pi\epsilon_0\} |\mathbf{x}|^3}. \quad (2.3)$$

Using the specification of \mathbf{x} in (2.1), we find

$$\begin{aligned} \Delta \mathbf{v}_{\perp} &= - \frac{Z_i e^2 b}{\{4\pi\epsilon_0\} m_e} (\hat{\mathbf{e}}_x \cos \varphi + \hat{\mathbf{e}}_y \sin \varphi) \int_{-\infty}^{\infty} \frac{dt}{(b^2 + v^2 t^2)^{3/2}} \\ &= - \frac{2Z_i e^2}{\{4\pi\epsilon_0\} m_e b v} (\hat{\mathbf{e}}_x \cos \varphi + \hat{\mathbf{e}}_y \sin \varphi). \end{aligned} \quad (2.4)$$

(This expression is relativistically correct if m_e is replaced by the relativistic mass $\gamma m_e = m_e / \sqrt{1 - v^2/c^2}$.) Note that the perturbation of the electron velocity is in a direction perpendicular to its direction of motion. There is no component along the direction of particle motion ($\hat{\mathbf{e}}_z$ direction), at least in this first order where the particle trajectory is the unperturbed one — because the z component of the Coulomb force is an odd function of z or t . Hence, to this first or lowest order there is no momentum loss by the particle. Rather, a typical electron is only deflected by a small angle $\Delta\vartheta \sim \Delta v_{\perp}/v \ll 1$ in velocity space. Using a typical impact parameter $b \sim n_e^{-1/3}$, the average inter-particle spacing in the plasma, and a typical electron speed $v \sim v_{Te}$, the typical deflection angle is $\Delta\vartheta \sim 1/[4\pi(n_e \lambda_D^3)^{2/3}] \ll 1$.

Since the background ion is at rest in the Lorentz collision model, electron energy is conserved during the elastic Coulomb collision process. Thus, we have $m_e |\mathbf{v}|^2/2 = m_e |\mathbf{v} + \Delta \mathbf{v}|^2/2 = m_e (|\mathbf{v}|^2 + 2\mathbf{v} \cdot \Delta \mathbf{v} + \Delta \mathbf{v} \cdot \Delta \mathbf{v})$, from which we find that the component of $\Delta \mathbf{v}$ parallel to \mathbf{v} can be determined from

$$\mathbf{v} \cdot \Delta \mathbf{v} = - \frac{1}{2} \Delta \mathbf{v} \cdot \Delta \mathbf{v} \simeq - \frac{1}{2} \Delta \mathbf{v}_{\perp} \cdot \Delta \mathbf{v}_{\perp}, \quad (2.5)$$

as indicated in Fig. 2.4. That is, because of electron energy conservation, the reduction in electron velocity along its direction of motion is given by half of the negative of the square of the perpendicular (\perp) deflection. The net velocity change along the $\hat{\mathbf{e}}_z$ or parallel (\parallel) direction of electron motion induced by a single Coulomb collision with a background ion is thus ($\mathbf{v} \cdot \Delta \mathbf{v} \equiv v \Delta v_{\parallel}$)

$$\Delta v_{\parallel} \simeq - \frac{1}{2v} \Delta \mathbf{v}_{\perp} \cdot \Delta \mathbf{v}_{\perp} = - \frac{2Z_i^2 e^4}{\{4\pi\epsilon_0\}^2 m_e^2 b^2 v^3}. \quad (2.6)$$

Note that while $\Delta \mathbf{v}_{\perp}$ is a first order quantity in terms of the weak Coulomb electric field between the two particles given in (2.2), Δv_{\parallel} is a second order quantity, as evidenced by the square of the $\{4\pi\epsilon_0\}$ factor in the denominator. The result in (2.6) can also be obtained directly by integrating the Coulomb electric field force along a perturbed (by the Coulomb collision) trajectory rather than the straight-line electron trajectory that was assumed in the preceding analysis — see Problem 2.5.

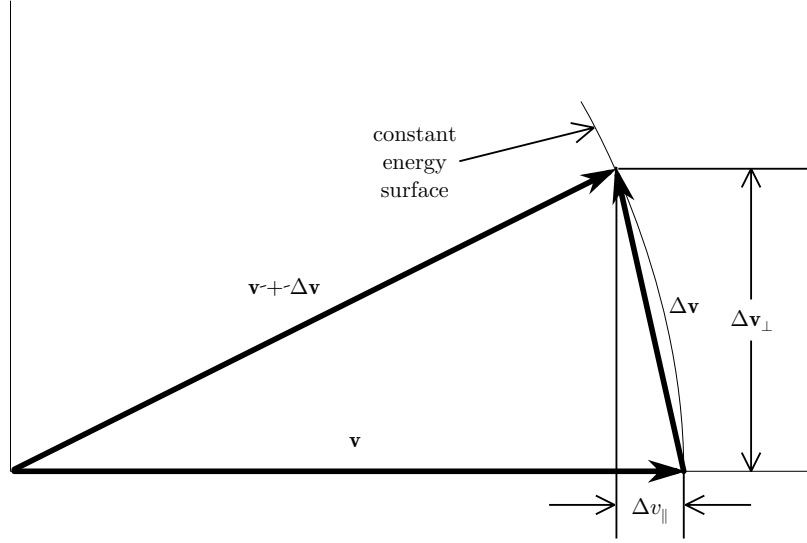


Figure 2.4: Change in electron velocity vector from \mathbf{v} before the Coulomb collision to $\mathbf{v} + \Delta\mathbf{v}$ afterward. The change takes place at constant electron energy, which means constant radius in this diagram, and hence results in $\Delta v_{\parallel} < 0$.

Next, we take account of the entire background distribution of ions, assuming that electron collisions with individual ions are statistically random and thus that their effects can be summed independently. For a density n_i of ions, adopting a cylindrical geometry in which the radius is b and the azimuthal angle is φ , the number of ions passed by the electron per unit time is $n_i \int d^3x/dt = n_i (dz/dt) \int dA = n_i v \int d\varphi \int b db$ (cf., Fig. 2.2). Hence, the net or ensemble average² Coulomb collisional force in the direction of electron motion is

$$\langle F_{\parallel} \rangle \equiv m_e \frac{\langle \Delta v_{\parallel} \rangle}{\Delta t} = n_i v \int_0^{2\pi} d\varphi \int_0^{\infty} b db m_e \Delta v_{\parallel} = - \frac{4\pi n_i Z_i^2 e^4}{\{4\pi\epsilon_0\}^2 m_e v^2} \int \frac{db}{b}. \quad (2.7)$$

Here, Δt is a typical interaction time for individual Coulomb collisions ($\Delta t \sim b/v \sim 1/[\omega_{pe}(n_e \lambda_D^3)^{1/3}]$), which is short compared to the time for the test electron to traverse a Debye sphere ($\sim \lambda_{De}/v \sim \lambda_{De}/v_{Te} \sim 1/\omega_{pe}$). It is also certainly short compared to the time scale on which the test particle velocity \mathbf{v} changes significantly due to Coulomb collisions [$\Delta t \ll 1/\nu$, where ν is the collision frequency defined in (2.14) below].

The integral over the impact parameter b in (2.7) is divergent at both its upper and lower limits: $\int_0^{\infty} db/b \Rightarrow \ln(\infty/0)$?! We restrict its range of in-

²In an ensemble average one averages over an infinite number of similar plasmas (“realizations”) that have the same number of particles and macroscopic parameters (e.g., density n , temperature T) but whose particle positions vary randomly from one realization to the next.

tegration through physical considerations that can be more rigorously justified by detailed analyses. The maximum impact parameter will be taken to be the Debye length since the Coulomb electric field force decays exponentially in space from the value given in (2.2) for distances larger than the Debye length (cf., Fig. ??):

$$b_{\max} = \lambda_D. \quad (2.8)$$

To estimate the minimum impact parameter b_{\min} , we note that when the Coulomb potential energy $q_e q_i / (\{4\pi\epsilon_0\}|\mathbf{x}|)$ becomes as large as the electron kinetic energy $m_e v^2/2$: Δv_{\parallel} becomes comparable to $|\Delta \mathbf{v}_{\perp}|$, the scattering angle becomes 90° [see (??) in Appendix A.1], and our weak interaction approximation breaks down. Hence, we determine a *classical minimum impact parameter* by $|\Delta v_{\parallel}| = |\Delta \mathbf{v}_{\perp}|$, which yields

$$b_{\min}^{\text{cl}} = \frac{Z_i e^2}{\{4\pi\epsilon_0\}(m_e v^2)} \simeq \frac{Z_i e^2}{\{4\pi\epsilon_0\}(3T_e)} = \frac{Z_i}{12\pi n_e \lambda_{De}^2} \simeq 4.8 \times 10^{-10} \frac{Z_i}{T_e(\text{eV})} \text{ m}. \quad (2.9)$$

Here, we have approximated $m_e v^2/2$ by $3T_e/2$, which is appropriate for a thermal electron in a Maxwellian distribution [cf., (??) in Appendix A.4].

Quantum mechanical effects become important when they could induce scattering through an angle ϑ of 90° , which occurs [for wave scattering processes — see (??) in Appendix A.7] when the distance of closest approach b is less than half the de Broglie wavelength $\lambda_h/2\pi \equiv \hbar/mv = h/(2\pi mv)$. This physical process yields a *quantum-mechanical minimum impact parameter*³ (for $v \simeq v_{Te} \equiv \sqrt{2T_e/m_e}$)

$$b_{\min}^{\text{qm}} \equiv \frac{\hbar}{2m_e v} \simeq \frac{h}{4\pi m_e v_{Te}} \simeq 1.1 \times 10^{-10} \frac{1}{T_e^{1/2}(\text{eV})} \text{ m}. \quad (2.10)$$

The relevant minimum impact parameter b_{\min} is the maximum of classical and quantum-mechanical minimum impact parameters. Quantum-mechanical effects dominate for $T_e \gtrsim 20 Z_i^2 \text{ eV}$. With these specifications of the limits of integration, the impact parameter integral in (2.7) can be written as

$$\ln \Lambda \equiv \int_{b_{\min}}^{b_{\max}} \frac{db}{b} = \ln \left(\frac{\lambda_D}{b_{\min}} \right), \quad b_{\min} = \max \{b_{\min}^{\text{cl}}, b_{\min}^{\text{qm}}\}, \quad \text{Coulomb logarithm.} \quad (2.11)$$

It is called the *Coulomb logarithm* because it represents the sum or cumulative effects of all Coulomb collisions within a Debye sphere for impact parameters ranging from b_{\min} to λ_D .

³In Chapter 13 of Jackson's *Classical Electrodynamics* the factor of 2 is omitted in the definition of the quantum-mechanical minimum impact parameter, but then the argument of the Coulomb logarithm in (2.11) is multiplied by a factor of 2 when quantum-mechanical effects dominate.

To determine the relative magnitude and scaling of Coulomb collision effects, it is convenient to assume classical effects determine the minimum impact parameter. When classical effects dominate ($b_{\min} = b_{\min}^{\text{cl}}$), the Coulomb logarithm becomes

$$\ln \Lambda^{\text{cl}} \equiv \ln \left(\frac{\lambda_D}{b_{\min}^{\text{cl}}} \right) \simeq \ln \left(\frac{12\pi n_e \lambda_{De}^3}{Z_i} \right). \quad (2.12)$$

Since the definition of a plasma (cf., Section 1.8) requires that $n_e \lambda_{De}^3 \gg \gg 1$, plasmas have $\ln \Lambda^{\text{cl}} \gg 1$. For example, typical magnetic fusion experiments in laboratory plasmas have $n \lambda_D^3 \sim 10^6$, and hence $\ln \Lambda \sim 17$.

Having defined the impact parameter integral in (2.7), the total Coulomb collisional force on a test electron along its direction of motion thus becomes

$$m_e \frac{dv_{\parallel}}{dt} = \langle F_{\parallel} \rangle = m_e \frac{\langle \Delta v_{\parallel} \rangle}{\Delta t} = - \left[\frac{4\pi n_i Z_i^2 e^4}{\{4\pi\epsilon_0\}^2 m_e^2 v^3} \ln \Lambda \right] m_e v_{\parallel} = -\nu m_e v_{\parallel}. \quad (2.13)$$

The Coulomb collisional drag force in the last form of this equation is called the *dynamical friction force* — because it is proportional to the test particle velocity. Here, we have defined a net momentum loss or slowing down⁴ Coulomb *collision frequency* for a particle of speed v in the Lorentz collision model:

$$\boxed{\nu(v) \equiv \frac{4\pi n_e Z_i e^4 \ln \Lambda}{\{4\pi\epsilon_0\}^2 m_e^2 v^3} \simeq \omega_{pe} \frac{\ln(12\pi n_e \lambda_{De}^3 / Z_i)}{4\pi n_e \lambda_{De}^3 / Z_i} \left(\frac{T_e}{m_e v^2} \right)^{3/2}} \quad (2.14)$$

Lorentz collision frequency.

In this definition we have taken into account the condition for quasineutrality in a plasma: $n_e = Z_i n_i$. Note from the last form in (2.14) that the electron collision frequency is smaller than the electron plasma frequency by a very large factor [$\propto 1/(n_e \lambda_{De}^3)$, which is by definition a small number in a plasma]. The Lorentz collision frequency can also be shown to be given by $\nu(v) = n_i \sigma_m v$ in which $\sigma_m = 4\pi (b_{\min}^{\text{cl}})^2 \ln \Lambda$ is a momentum transfer cross-section — see Problems 2.6, 2.7. It can also be deduced from the Langevin equation in which the stochastic force is due to Coulomb collisions — see Problem 2.8.

For classical “hard” collisions with $b < b_{\min}^{\text{cl}}$, the maximum parallel momentum transfer is given by $\max(\Delta v_{\parallel}) = 2v$. The collision frequency for hard collisions can be estimated using a cross section of $\sigma_{\text{hard}} \simeq \pi (b_{\min}^{\text{cl}})^2$: $\nu_{\text{hard}} = n_i \sigma_{\text{hard}} \max(\Delta v_{\parallel}) \simeq 2\pi n_i v (b_{\min}^{\text{cl}})^2$, which is smaller than the collision frequency in (2.14) by a factor of $1/(2 \ln \Lambda) \ll 1$. Thus, the net Coulomb collision frictional force is dominated by the *cumulative small angle collisions* with impact parameters b ranging between b_{\min} and λ_D that are embodied in the $\ln \Lambda$ integral in (2.11). That is, the Coulomb logarithm represents the degree to which cumulative small-angle collisions dominate over hard collisions for Coulomb collision processes in plasmas.

⁴Note that in the Lorentz collision model there is no energy transfer and only loss of directed momentum — see Problem 2.4. It is thus unfortunate and rather misleading that the Lorentz collision frequency is often called a “slowing down” frequency in plasma physics.

Detailed treatments of the physical phenomena of hard collisions for $b \leq b_{\min}$ (see Problems 2.7, 2.24) and of the Debye shielding process (see Chapter 13) for $b \gtrsim b_{\max} = \lambda_D$ yield order unity corrections to the $\ln \Lambda \equiv \ln(b_{\max}/b_{\min})$ factor in (2.14). However, because these corrections are small and quite complicated, it is customary to neglect them in most plasma physics calculations. Thus, the Coulomb collision momentum loss frequency given in (2.14) and the other Coulomb collision processes calculated in this chapter should be assumed to be accurate to within factors of order $1/(\ln \Lambda) \sim 5 - 10\%$; evaluation of Coulomb collision processes and their effects to greater accuracy is unwarranted.

Finally, we use our result for the Coulomb collision frictional force $\langle F_{\parallel} \rangle$ on a single electron to calculate the net frictional force on a “drifting” Maxwellian distribution of electrons flowing slowly (compared to their thermal speed) through a background of fixed, immobile ions. For a small net flow speed V_{\parallel} in the $\hat{\mathbf{e}}_z$ direction, the appropriate *flow-shifted Maxwellian distribution* for electrons is⁵

$$\begin{aligned} f_{Me}(\mathbf{v}) &= n_e \left(\frac{m_e}{2\pi T_e} \right)^{3/2} \exp \left(- \frac{m_e |\mathbf{v} - V_{\parallel} \hat{\mathbf{e}}_z|^2}{2T_e} \right) \\ &\simeq n_e \left(\frac{m_e}{2\pi T_e} \right)^{3/2} e^{-m_e v^2/2T_e} \left[1 + \frac{m_e v_{\parallel} V_{\parallel}}{T_e} + \dots \right] \\ &= \frac{n_e e^{-v^2/v_{Te}^2}}{\pi^{3/2} v_{Te}^3} \left[1 + \frac{2 v_{\parallel} V_{\parallel}}{v_{Te}^2} + \dots \right], \end{aligned} \quad (2.15)$$

in which in the last form we have used the convenient definition of the electron thermal speed $v_{Te} \equiv \sqrt{2T_e/m_e}$. Multiplying (2.13) by this distribution and integrating over the relevant spherical velocity space ($v_{\parallel} \equiv v \zeta = v \cos \vartheta$), the Maxwellian-average (indicated by a bar over F_{\parallel}) of the Coulomb collisional frictional force density on the drifting electron fluid becomes

$$\begin{aligned} n_e \langle \bar{F}_{\parallel} \rangle &\equiv \int d^3v f_{Me}(\mathbf{v}) \langle F_{\parallel} \rangle \\ &\equiv - \int_0^{2\pi} d\varphi \int_{-1}^1 d\zeta \int_0^{\infty} v^2 dv \nu(v) m_e v \zeta \frac{2v\zeta V_{\parallel}}{v_{Te}^2} \frac{n_e e^{-v^2/v_{Te}^2}}{\pi^{3/2} v_{Te}^3} \\ &= -\nu_e m_e n_e V_{\parallel}. \end{aligned} \quad (2.16)$$

Here, we have defined the Maxwellian-averaged electron-ion collision frequency

$$\boxed{\nu_e \equiv \frac{4}{3\sqrt{\pi}} \nu(v_{Te}) = \frac{4\sqrt{2\pi} n_i Z_i^2 e^4 \ln \Lambda}{\{4\pi\epsilon_0\}^2 3 m_e^{1/2} T_e^{3/2}} \simeq \frac{5 \times 10^{-11} n_e Z_i}{[T_e(\text{eV})]^{3/2}} \left(\frac{\ln \Lambda}{17} \right) \text{s}^{-1}},} \quad \text{fundamental electron collision frequency.} \quad (2.17)$$

This is the average momentum relaxation rate for the slowly flowing Maxwellian distribution of electrons. Since many transport processes arise from collisional

⁵Here, and throughout this text, a capital letter V (\mathbf{V}) will indicate the average flow speed (velocity) of an entire species of particles while a small letter v (\mathbf{v}) will indicate the speed (velocity) of a particular particle, or a particular position in velocity space.

relaxations of flows in a plasma, this average or reference electron collision frequency is often the fundamental collision frequency that arises — in the plasma electrical conductivity (see Section 2.3 below) and plasma transport studies (cf., Problem 2.10).

Since a typical, thermal electron moves at the thermal speed v_{Te} , it is convenient to define the characteristic length scale over which the momentum in a flowing distribution of electrons is damped away by

$$\lambda_e \equiv \frac{v_{Te}}{\nu_e} \simeq 1.2 \times 10^{16} \frac{[T_e(\text{eV})]^2}{n_e Z_i} \left(\frac{17}{\ln \Lambda} \right), \quad \text{electron collision length.} \quad (2.18)$$

Note that (in contrast to neutral particle collisions) it is not appropriate to call this length a collision “mean free path” — because a very large number of random small-angle Coulomb collisions deflect particles’ velocities and cause the net momentum loss over this length scale. [The total number of collisions involved is of order $n\lambda_D^3$ as a test electron traverses a Debye length times a factor of $\lambda_e/\lambda_D \simeq n\lambda_D^3/\ln \Lambda$, or of order $(n\lambda_D^3)^2/\ln \Lambda \gg \gg \gg \gg 1$.] For the relevant length and time scales in some typical plasmas, see Problems 2.1–2.3

2.2 Diffusive Properties of Coulomb Collisions

The Coulomb collision process causes more than just momentum loss by the electrons. As indicated in Fig. 2.4, the dominant collisional process in individual collisions is deflection of the test particle velocity in a random direction perpendicular to the original direction of motion. The net perpendicular Coulomb collision force defined analogously to the net parallel force in (2.7) vanishes:

$$\langle \mathbf{F}_\perp \rangle \equiv m \frac{\langle \Delta \mathbf{v}_\perp \rangle}{\Delta t} = n_i v \int_0^{2\pi} d\varphi \int_{b_{\min}}^{b_{\max}} b db m_e \Delta \mathbf{v}_\perp = \mathbf{0}.$$

While the ensemble average perpendicular force vanishes, because of the randomness of the impact angle φ , velocity-space deflections caused by Coulomb collisions do have an effect in the perpendicular direction. Namely, they lead to diffusion of the test particle velocity \mathbf{v} in directions perpendicular to \mathbf{v} . For a general discussion of diffusive processes see Appendix A.5.

The temporal evolution of the velocity of a test particle as it undergoes random Coulomb collisions with background ions is illustrated in Fig. 2.5. While for long times (many Coulomb collisions) the average of the perpendicular velocity component v_x vanishes ($\langle v_x \rangle = 0$), its square and the reduction of the velocity component in the original direction of motion increase approximately linearly with time — $\langle v_x^2 \rangle \simeq (\langle \Delta v_x^2 \rangle / \Delta t) t$ [see (??) in Appendix A.5] and $v_0 - v_z \sim (\langle \Delta v_\parallel \rangle / \Delta t) t$. The fact that the average of v_x^2 increases linearly with time while the average of v_x vanishes indicates a diffusive process for the x (perpendicular) component of the test particle velocity — see Appendix A.5. Because there is no preferred direction in the plane perpendicular to the original direction of

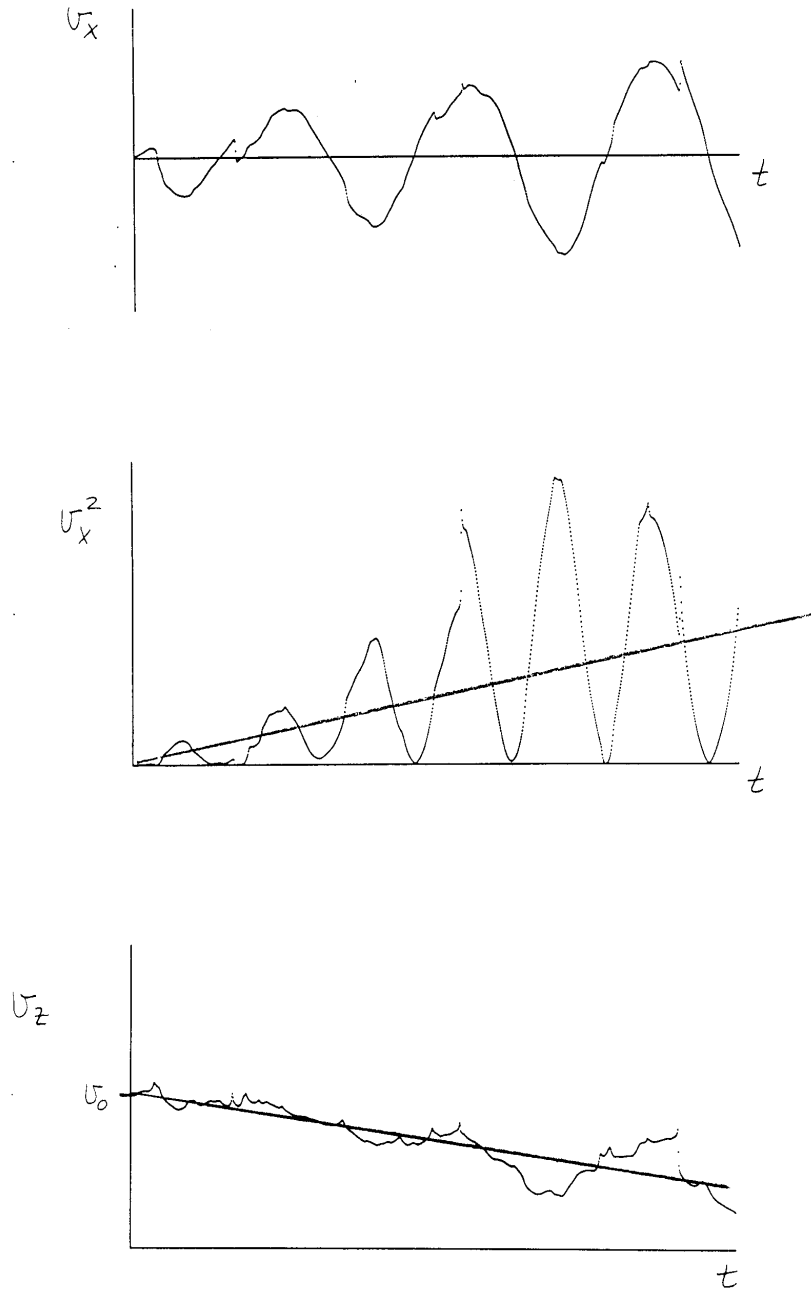


Figure 2.5: Temporal evolution of v_x , v_x^2 and v_z components of the test particle velocity as it undergoes random Coulomb collisions with background ions. Note that for times long compared to an individual Coulomb collision time the average of v_x vanishes, but v_x^2 and $v_0 - v_z$ increase approximately linearly with time t .

motion, we obtain $\langle v_x^2 \rangle = \langle v_y^2 \rangle = \langle v_\perp^2 \rangle / 2 = (1/2) \langle \Delta v_\perp^2 \rangle / \Delta t$; hence there is velocity diffusion equally in both the x and y directions.

To mathematically describe the diffusion in velocity space, we calculate the mean square deflection of the test electron as it moves through the background ions by the same ensemble-averaging procedure as that used in obtaining the average parallel force in (2.7). We obtain

$$\frac{\langle \Delta v_\perp^2 \rangle}{\Delta t} \equiv n_i v \int_0^{2\pi} d\varphi \int_{b_{\min}}^{b_{\max}} b db \Delta \mathbf{v}_\perp \cdot \Delta \mathbf{v}_\perp = \frac{8\pi n_i Z_i^2 e^4}{\{4\pi\epsilon_0\}^2 m^2 v} \ln \Lambda = 2\nu v^2. \quad (2.19)$$

Thus, as can be inferred from (2.5), and from Figs. 2.4 and 2.5, in the Lorentz scattering model the rate of velocity diffusion ($\langle \Delta v_\perp^2 \rangle / v^2 \Delta t$) for the test electron is twice the rate of momentum loss ($\langle \Delta v_\parallel \rangle / v \Delta t$). Note that for the collisional process being considered the velocity diffusion takes place at constant energy and in directions perpendicular to the test particle velocity \mathbf{v} ; there is no speed (energy) diffusion in the Lorentz collision model because the background particles (ions here) are assumed to be immobile and hence to not exchange energy with the test electron.

In the spherical velocity space we are using, the “pitch-angle” through which the random scattering, deflections and diffusion take place is defined by $\sin \vartheta \equiv v_\perp / v = \sqrt{v_x^2 + v_y^2} / v$. Since the Coulomb collision process is a random walk or diffusion process (in pitch-angle), the time required to diffuse the test particle velocity vector through a small angle $\vartheta \simeq v_\perp / v \ll 1$ is much less than the Lorentz collision model (momentum loss) time $1/\nu$, which is effectively the time scale for scattering through 90° — see Problem 2.12 for a specific example. From (2.19) we can infer that collisional scattering through an angle $\vartheta \ll 1$ (but ϑ must be greater than the $\Delta\vartheta$ for any individual Coulomb interaction so a diffusive description applies) occurs in a time [see Fig. 2.5 and (??)]

$$t \sim (v_\perp / v)^2 / \nu \sim \vartheta^2 / \nu \ll 1/\nu, \quad \text{time to diffuse through } \vartheta \ll 1. \quad (2.20)$$

As time progresses, a test particle’s “pitch-angle” ϑ in velocity space is randomly deflected or scattered. Thus, over time the pitch-angle of a test particle assumes a probability distribution whose width is given by $\sqrt{\langle \vartheta^2 \rangle} \sim \sqrt{\nu t}$.

For the Lorentz collision model the probability distribution of a test particle with an initial velocity \mathbf{v}_0 [i.e., $f(\mathbf{v}, t = 0) \equiv \delta(\mathbf{v} - \mathbf{v}_0)$] can be shown (see Section 11.2) to be given for short times by

$$f_t(v, \vartheta, t) \simeq \frac{\delta(v - v_0)}{2\pi v_0^2} \left(\frac{e^{-\vartheta^2/2\nu t}}{\nu t} \right) = \frac{\delta(v - v_0)}{2\pi v_0^2} \left(\frac{e^{-v_\perp^2/(2v^2\nu t)}}{\nu t} \right) \quad \text{for } \nu t \ll 1. \quad (2.21)$$

This distribution function is normalized so it represents one test particle: i.e., $\int d^3v f_t = 1$. The delta function in speed, $\delta(v - v_0)$, represents the fact that

the test particle speed stays constant at the initial speed $|\mathbf{v}_0| \equiv v_0$ — because the test particle energy (speed) is constant in the Lorentz collision model. The factor $e^{-\vartheta^2/2\nu t}/(\nu t)$ represents the diffusion in pitch-angle ϑ that takes place in a time t ; it indicates that f_t is reduced by a factor of $e^{-1/2} \simeq 0.61$ for diffusion over a pitch-angle of $\vartheta \ll 1$ in the short time $t \sim \vartheta^2/\nu$ indicated in (2.20). The velocity-space diffusion properties of Coulomb collision processes are explored in greater detail in Chapter 11.

The dynamical friction and diffusion coefficients for the Lorentz collision model can be written in a coordinate-independent, vectorial form as follows. First, note that the parallel or z direction here is defined to be in the initial electron velocity direction: $\hat{\mathbf{e}}_z \equiv \mathbf{v}/v$. Thus, we can write the dynamical friction force coefficient due to Coulomb collisions in the form

$$\boxed{\frac{\langle \Delta \mathbf{v} \rangle}{\Delta t} = \frac{\langle \Delta v_{\parallel} \rangle}{\Delta t} \hat{\mathbf{e}}_z = -\nu(v) \mathbf{v}.} \quad (2.22)$$

Similarly, because velocity diffusion occurs equally in all directions perpendicular to \mathbf{v} , we have $\langle \Delta v_x^2 \rangle / \Delta t = \langle \Delta v_y^2 \rangle / \Delta t = (1/2) \langle \Delta v_{\perp}^2 \rangle / \Delta t$; hence the (second rank tensor) diffusion coefficient can be written as

$$\boxed{\frac{\langle \Delta \mathbf{v} \Delta \mathbf{v} \rangle}{\Delta t} = \frac{1}{2} \frac{\langle \Delta v_{\perp}^2 \rangle}{\Delta t} (\hat{\mathbf{e}}_x \hat{\mathbf{e}}_x + \hat{\mathbf{e}}_y \hat{\mathbf{e}}_y) = \nu(v) (v^2 \mathbf{I} - \mathbf{v} \mathbf{v}),} \quad (2.23)$$

in which \mathbf{I} is the identity tensor [see (??) in Appendix D.7]. These forms for $\langle \Delta \mathbf{v} \rangle / \Delta t$ and $\langle \Delta \mathbf{v} \Delta \mathbf{v} \rangle / \Delta t$ will be useful in Section 11.1 where we will develop a Lorentz Coulomb collision operator for use in plasma kinetic theory.

2.3 Runaway Electrons and Plasma Resistivity

Next, we consider the combined effects of a macroscopic electric field \mathbf{E} and the dynamical friction due to Coulomb collisions on test electrons in a plasma. Using the dynamical friction force given in (2.13) using the vectorial form indicated in (2.22), Newton's second law for this situation can be written in the form

$$m_e \frac{d\mathbf{v}}{dt} = q_e \mathbf{E} - \nu m_e \mathbf{v}. \quad (2.24)$$

The electric field may be externally imposed, or arise from a collective response in the plasma. The electric field \mathbf{E} , which we take to be in the $-\hat{\mathbf{e}}_z$ direction accelerates electrons ($q_e = -e$) in the $-\mathbf{E}$ or $+\hat{\mathbf{e}}_z$ direction; Coulomb collisions exert a dynamical friction force that opposes this acceleration. In a more complete Coulomb collision model that includes electron-electron collisions (see Section 2.7 below), the Lorentz collision frequency ν gets replaced by a “slowing down” (subscript S) electron (momentum relaxation) collision frequency $\nu_S^e = \nu_S^{e/e} + \nu_S^{e/i}$, in which $\nu_S^{e/e}$ and $\nu_S^{e/i}$ are the momentum loss rates for electron-electron and electron-ion collisions, which will be derived explicitly

below, in Section 2.9. For electron-ion collisions, since electron speeds are typically much greater than the ion thermal speed and little energy is transferred during the collisions because of the large disparity in masses, the ions are essentially immobile during the Coulomb collision process. Thus, the Lorentz collision model is applicable and the relevant electron-ion collision frequency is simply the Lorentz collision frequency: $\nu_S^{e/i} = \nu(v)$, as given in (2.14). Electron-electron collisions are in general more complicated — because during collisions both particles are in motion and energy is transferred. With these simplifications and adaptations, the equation governing the velocity of a single electron in the $\hat{\mathbf{e}}_z$ direction, (2.24) can be rewritten in the more precise one-dimensional form

$$m_e \frac{dv_{\parallel}}{dt} = (-e)(-E) - (\nu_S^{e/e} + \nu_S^{e/i}) m_e v_{\parallel} = eE - \nu_S^e m_e v_{\parallel}. \quad (2.25)$$

We first consider the combined electric field and Coulomb collision effects on energetic test electrons in the high energy tail of a Maxwellian distribution. For these energetic test electrons the background electrons can be considered at rest and the electron-electron momentum loss collision frequency is simply $\nu_S^{e/e} = 2\nu(v)/Z_i$ (see Table 2.1) — the factor of two comes from the inverse dependence on the reduced electron rest mass [see (2.55) below] and the $1/Z_i$ factor eliminates the dependence on the ion Z_i in the Lorentz model collision frequency. The total momentum loss collision frequency for these energetic electrons can thus be written as

$$\nu_S^e = (1 + 2/Z_i) \nu(v) = (1 + 2/Z_i) \nu(v_{Te}) v_{Te}^3 / v^3, \quad \text{for } v \gg v_{Te}. \quad (2.26)$$

Here, the unity multiplicative factor (on ν) represents electron-ion collisions and the $2/Z_i$ factor represents electron-electron collisions. In the limit $Z_i \gg 2$ this overall electron momentum relaxation rate becomes simply the Lorentz model collision frequency and electron-electron collision effects are negligible.

The dynamical friction force $\nu_S^e(v) m_e v_{\parallel}$ in (2.25) with the ν_S^e given in (2.26) decreases as v^{-2} for electrons in the high energy tail of a Maxwellian distribution. The dependence of the electric field and dynamical friction forces on the speed v of a tail electron are illustrated in Fig. 2.6. As indicated, when the electric field force exceeds the dynamical friction force, electrons are freely accelerated by the electric field. Such electrons are called *runaway electrons*. The energy range for which runaway electrons occur is determined by $eE > \nu_S^e m_e v$:

$$\frac{m_e v^2}{2T_e} > (2 + Z_i) \frac{E_D}{|\mathbf{E}|}, \quad (2.27)$$

where

$$E_D \equiv \frac{2\pi n_e e^3 \ln \Lambda}{\{4\pi\epsilon_0\}^2 T_e} = \frac{e (\frac{1}{2} \ln \Lambda)}{\{4\pi\epsilon_0\} \lambda_{De}^2} = \frac{m_e v_{Te} \nu(v_{Te})}{e Z_i}, \quad \text{Dreicer field} \quad (2.28)$$

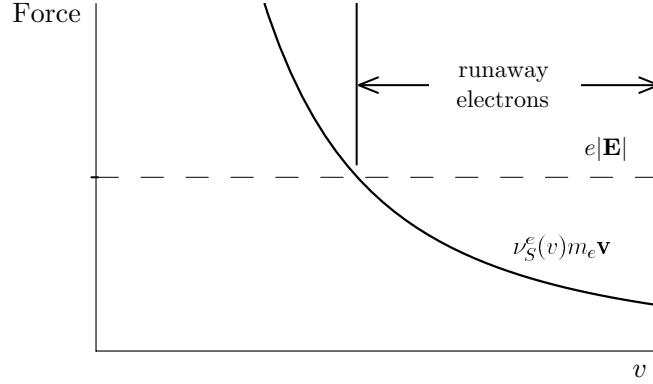


Figure 2.6: Relative strengths of the electric field $e|\mathbf{E}|$ and dynamical friction $\nu_S^e(v) m_e \mathbf{v}$ forces on an electron as a function of the electron speed v . Runaway electrons occur when the electric field force exceeds the dynamical friction force.

is a critical electric field strength, called the *Dreicer field*.⁶ For weak electric fields ($|\mathbf{E}| \ll E_D$), the energy at which electron runaways occur is far out on the high energy tail of the Maxwellian electron distribution and only an exponentially small fraction of electrons run away — see Problem 2.13. [For relativistic electron energies the dynamical friction decreases less rapidly than $1/v^2$ and no runaways are produced for a weak electric field satisfying $|\mathbf{E}|/E_D < 2T_e/(m_e c^2)$ — see Problem 2.14.] High Z_i ions increase the energy for electron runaway relative to that for protons — because they increase the frictional drag due to Coulomb collisions. Note also from the middle form of the critical electric field defined in (2.28) that its magnitude is roughly (to within a factor of $\frac{1}{2} \ln \Lambda \sim 10$) what is required to substantially distort the Coulomb electric field around a given ion [cf., (2.2)] at distances of order the Debye length. Alternatively, it can be seen from the last form in (2.28) that the Dreicer field is approximately the electric field strength at which typical, thermal energy electrons with $v \sim v_{Te}$ in a Maxwellian distribution become runaways — see Problem 2.15 for a more precise estimate. Thus, when the electric field is larger than the Dreicer field, the entire distribution of electrons responds primarily to the electric field and collisional effects are small.

For weak electric fields $|\mathbf{E}| \ll E_D$, most plasma electrons will be only slightly accelerated by the \mathbf{E} field before Coulomb collisions relax the momentum they gain. However, the velocity distribution of electrons will acquire a net flow velocity \mathbf{V}_e in response to the \mathbf{E} field. Since the more massive ions have much more inertia and are accelerated less by the electric field, they acquire a much

⁶H. Dreicer, *Proceedings of the Second United Nations International Conference on the Peaceful Use of Atomic Energy* (United Nations, Geneva, 1958), Vol. 31, p. 57. See also, *Phys. Rev.* **115**, 238 (1959).

smaller [by a factor $\sim (m_e/m_i)^{1/2} \lesssim 1/43 \ll 1$] flow, which can be neglected. Thus, the electron flow in response to the electric field will correspond to an electric current flowing in the plasma. The proportionality constant between the current and electric field is the plasma electrical conductivity, which we will now determine.

For electrons with a flow-shifted Maxwellian distribution as in (2.15) that have a flow velocity \mathbf{V}_e relative to the ions ($V_{\parallel} \hat{\mathbf{e}}_z \rightarrow \mathbf{V}_e - \mathbf{V}_i$), the average (over the Maxwellian distribution) frictional force is given in (2.16). Adding electric field force and electron inertia effects yields the electron momentum density equation

$$m_e n_e \frac{d\mathbf{V}_e}{dt} = -en_e \mathbf{E} - m_e n_e \nu_e (\mathbf{V}_e - \mathbf{V}_i), \quad (2.29)$$

in which ν_e is the fundamental electron collision frequency defined in (2.17). In equilibrium ($t \gg 1/\nu_e$, $d/dt \rightarrow 0$) we obtain the current induced by an electric field:

$$\mathbf{J} = -n_e e (\mathbf{V}_e - \mathbf{V}_i) = \sigma_0 \mathbf{E}, \quad \text{Ohm's law} \quad (2.30)$$

in which

$$\sigma_0 = \frac{n_e e^2}{m_e \nu_e} \equiv \frac{1}{\eta}, \quad \text{reference (subscript 0) plasma electrical conductivity,}$$

(2.31)

where η is the plasma resistivity. The electron collision frequency that enters this formula is ν_e , which is the (electron-ion) Lorentz collision frequency (2.14) averaged over a flowing Maxwellian distribution of electrons given in (2.17). (In this analysis the electron Coulomb collision frequency is assumed to be much greater than the electron-neutral collision frequency. See Problems 2.19, 2.20 for situations where this assumption is not valid and the electrical conductivity is modified.) Note also that since $n_e/\nu_e \propto T_e^{3/2}$, the electrical conductivity in a plasma increases as $T_e^{3/2}$ — an inverse dependence compared to solid conductors whose electrical conductivity decreases with temperature. The conductivity in plasmas increases with electron temperature because the noise level [see (??)] and collision frequency [see (2.17)] decrease with increasing electron temperature and Debye length. For some perspectives on the magnitude and effects of the electrical conductivity in plasmas, see Problems 2.16–2.18.

In a more complete, kinetic analysis with the Lorentz collision model (see Section 11.4), the electric field distorts the electron distribution function more than indicated by the simple flow effect in (2.15). Specifically, we can infer from (2.25) and (2.26) that higher energy electrons receive larger momentum input from the electric field because the Coulomb collision dynamical friction force decreases as v^{-2} . Thus, the current is carried mainly by higher energy ($v \sim 2v_{Te}$), lower collisionality electrons than is embodied in the simple flow-shifted Maxwellian distribution. Since the collision frequency decreases as $1/v^3$,

the Maxwellian-averaged collision frequency is reduced (see Section 11.4), by a factor of $3\pi/32 \simeq 0.2945 \equiv \alpha_e$; thus the electrical conductivity in a kinetic Lorentz model is increased relative to that given in (2.31) by the factor $1/\alpha_e$.

Electron-electron collisions are momentum conserving for the electron distribution function as a whole. Thus, they do not contribute directly to the momentum loss process or plasma electrical conductivity. However, in a kinetic description the electric field distorts the electron distribution function away from a flow-shifted Maxwellian. Then, electron-electron collisions have an indirect effect of reducing the net flow (and electrical conductivity) in response to an electric field — as they try to force the electron distribution to be close to a Maxwellian. Details of this process will be discussed in Section 12.3.

The net result of these kinetic and electron-electron effects, which is obtained from a complete, kinetic analysis that was first solved numerically by Spitzer and Härm,⁷ is that the effective electron collision frequency is reduced by a generalized factor α_e . Thus, the electrical conductivity becomes

$$\boxed{\sigma_{Sp} = \frac{n_e e^2}{m_e \alpha_e \nu_e} = \frac{\sigma_0}{\alpha_e}, \quad \text{Spitzer electrical conductivity.}} \quad (2.32)$$

The generalized factor α_e ranges from 0.5129 for $Z_i = 1$ to $3\pi/32 \simeq 0.2945$ for $Z_i \rightarrow \infty$ (Lorentz kinetic model). A later analytic fluid moment analysis⁸ has shown that this factor can be approximated to three significant figures (see Section 12.3), which is much more accuracy than warranted by the intrinsic accuracy ($\sim 1/\ln \Lambda \lesssim 10\%$) of the Coulomb collision operator, by

$$\alpha_e \simeq \frac{1 + 1.198Z_i + 0.222Z_i^2}{1 + 2.966Z_i + 0.753Z_i^2}. \quad (2.33)$$

2.4 Effects of Coulomb Collisions

So far we have concentrated on the electron momentum relaxation effects of Coulomb collisions using a Lorentz collision model. In this section we discuss phenomenologically more general Coulomb collision effects on electrons as well as the collisional effects on ions, and between ions and electrons. A complete, rigorous treatment of Coulomb collision effects begins in Section 2.6.

The Lorentz collision model takes into account electron-ion collisions but neglects electron-electron collisions. However, these two collisional processes occur on approximately the same time scale, at least for ions with a Z_i that is not too large. As indicated in the preceding section, electron-electron collisions tend to relax the electron velocity distribution toward a Maxwellian distribution function. They do so on approximately the fundamental electron collision time scale $1/\nu_e$. However, as indicated in (2.25) and (2.26), the collisional relaxation of electrons in the high energy tail of the distribution is slower. The characteristic time τ for tail electrons to equilibrate toward a Maxwellian distribution is

⁷L. Spitzer and R. Härm, Phys. Rev. **89**, 977 (1953).

⁸S.P. Hirshman, Phys. Fluids **20**, 589 (1977).

$\tau \sim (v/v_{Te})^3/\nu_e$ for $v \gg v_{Te}$. (For an application where this effect is important see Problem 2.21.) In contrast, all electrons with $v \lesssim v_{Te}$ relax toward a Maxwellian distribution on the same time scale as the bulk (see Section 2.7 and Problem 2.32): $\tau \sim 1/\nu_e$.

As indicated in (2.16) and (2.29), the net Coulomb collisional force density on a Maxwellian distribution of electrons flowing relative to the ions is

$$\mathbf{R}_e \equiv -m_e n_e \nu_e (\mathbf{V}_e - \mathbf{V}_i) = \frac{n_e e \mathbf{J}}{\sigma}, \quad \text{collisional friction force density.} \quad (2.34)$$

This is the electron force density that was introduced in the electron fluid momentum balance given in (2.29). Note also from a temporal solution of (2.29) that the electron flow (momentum) will relax exponentially to its equilibrium value at the rate ν_e , i.e., on the electron time scale $\tau_e = 1/\nu_e$. Because Coulomb collisions are momentum conserving, any momentum lost from the electrons must be gained by the ions. Thus, the Coulomb collisional force density on ions is given by

$$\mathbf{R}_i = -\mathbf{R}_e. \quad (2.35)$$

Ion-ion collisions are analogous to electron-electron collisions and complicated — during Coulomb collisions both particles are in motion and energy is exchanged between them. Nonetheless, considering a Lorentz-type model for ion-ion collisions using the framework developed in Section 2.1, it is easy to see that the appropriate ion collision frequency should scale inversely with the square of the ion mass and the cube of the ion speed. A detailed analysis (see Sections 2.6–2.10) of the effects of ion-ion collisions yields a flowing-Maxwellian-averaged ion collision frequency given by

$$\nu_i = \frac{4\sqrt{\pi} n_i Z_i^4 e^4 \ln \Lambda}{\{4\pi\epsilon_0\}^2 3 m_i^{1/2} T_i^{3/2}} = \left(\frac{m_e}{m_i}\right)^{1/2} \left(\frac{T_e}{T_i}\right)^{3/2} \frac{Z_i^2}{\sqrt{2}} \nu_e, \quad (2.36)$$

fundamental ion collision frequency.

The $\sqrt{2}$ factor (in the denominator at the end of the second formula) enters because of the combined effects of the reduced mass [see (2.55) below] and the motion of both particles during ion-ion collisions. Note that for an electron-proton ($Z_i = 1$) plasma with $T_e \sim T_i$ the ion collision frequency is smaller than the electron collision frequency by a square root of the mass ratio: $\nu_i/\nu_e \sim (m_e/2m_i)^{1/2} \lesssim 1/60 \ll 1$. Because of their very disparate masses, ion-electron collisional effects are typically smaller than ion-ion collisional effects by a factor of $(m_e/m_i)^{1/2} \lesssim 1/43 \ll 1$; hence they are negligible for ion collisional effects. As for electrons, ion collisions drive the velocity distribution of ions toward a Maxwellian distribution on the ion collisional time scale $\tau_i = 1/\nu_i \sim (2m_i/m_e)^{1/2}/\nu_e \gg 1/\nu_e$. In addition, like electrons, ions in the high energy tail of the distribution relax toward a Maxwellian distribution more slowly: $\tau \sim (v/v_{Ti})^3/\nu_i$ for $v \gg v_{Ti}$.

We now determine the small energy transfer from electrons to ions during Coulomb collisions, which we have heretofore neglected. Momentum is conserved during a Coulomb collision. Thus, if an electron acquires an impulse $m_e \Delta \mathbf{v}_e$ during an electron-ion collision, the ion acquires an impulse determined from momentum conservation:

$$m_e \Delta \mathbf{v}_e + m_i \Delta \mathbf{v}_i = \mathbf{0} \implies \Delta \mathbf{v}_i = - (m_e/m_i) \Delta \mathbf{v}_e.$$

The energy exchange from electrons to ions initially at rest during a Coulomb collision will thus be

$$\frac{m_i}{2} \Delta \mathbf{v}_i \cdot \Delta \mathbf{v}_i = \frac{m_i}{2} \left(\frac{m_e}{m_i} \right)^2 \Delta \mathbf{v}_e \cdot \Delta \mathbf{v}_e \simeq \left(\frac{m_e}{m_i} \right) \frac{m_e}{2} \Delta v_\perp^2.$$

The net energy exchange from a test electron moving through the background stationary ions can thus be evaluated using (2.19):

$$\frac{m_i}{2} \frac{\langle \Delta \mathbf{v}_i \cdot \Delta \mathbf{v}_i \rangle}{\Delta t} = \left(\frac{m_e}{m_i} \right) m_e v^2 \nu(v). \quad (2.37)$$

Note that this energy exchange rate is smaller than the basic Lorentz collision frequency ν by a factor of $m_e/m_i \lesssim 10^{-3} \ll 1$ — because lightweight electrons transfer very little energy to the massive ions in Coulomb collisions.

Integrating this last result over a Maxwellian distribution of the electrons, the Maxwellian-averaged rate of energy (ε) density transfer from electrons to initially stationary background ions ($\equiv \bar{\nu}_\varepsilon^{e/i}$ in Section 2.10) becomes

$$\int d^3v f_{Me} \frac{m_i}{2} \frac{\langle \Delta \mathbf{v}_i \cdot \Delta \mathbf{v}_i \rangle}{\Delta t} \equiv \bar{\nu}_\varepsilon^{e/i} n_e T_e = 3 \frac{m_e}{m_i} \nu_e n_e T_e.$$

A more complete analysis (see Section 2.10) shows that if the background ions have a Maxwellian velocity distribution (instead of being stationary and immobile as they are in the Lorentz model) $T_e \rightarrow T_e - T_i$ in this formula, as would be expected physically. Thus, the rate of ion energy density increase from Coulomb collisions with electrons is

$$Q_i \equiv \bar{\nu}_\varepsilon^{e/i} n_e (T_e - T_i) = 3 \frac{m_e}{m_i} \nu_e n_e (T_e - T_i), \quad \text{ion collisional heating density.}$$

(2.38)

In the absence of other effects, the equation governing ion temperature evolution becomes

$$\frac{3}{2} n_i \frac{dT_i}{dt} = Q_i = 3 \frac{m_e}{m_i} \nu_e n_e (T_e - T_i). \quad (2.39)$$

Here, $(3/2)(n_i dT_i/dt)$ represents the rate of increase of ion internal energy in the plasma. From (2.39) we see that for a constant electron temperature the characteristic time scale on which Coulomb collisions equilibrate the ion temperature

to the electron temperature is $\tau_{i-e} = 3/(2\bar{\nu}_{\varepsilon}^{e/i}) = (m_i/2m_e)/\nu_e \gtrsim 10^3/\nu_e \gg 1/\nu_e$. (For a more precise determination of the temporal evolution of the collisional equilibration of the electron and ion temperatures in a plasma, see Problem 2.23.)

Because energy is conserved in the elastic Coulomb collisions, energy gained by the ions is lost from the electrons. In addition, the electrons are heated by the work they do per unit time in flowing relative to the ions against the collisional friction force density \mathbf{R}_e given in (2.34). Thus, the total electron heating due to Coulomb collisions is given by

$$Q_e = -(\mathbf{V}_e - \mathbf{V}_i) \cdot \mathbf{R}_e - Q_i = J^2/\sigma - Q_i. \quad (2.40)$$

In the absence of other effects and using $1/\sigma = \eta$, the electron temperature evolution equation becomes

$$\frac{3}{2} n_e \frac{dT_e}{dt} = Q_e = \eta J^2 - Q_i. \quad (2.41)$$

In these equations ηJ^2 is the joule or ohmic heating induced by a current density \mathbf{J} flowing in a plasma with resistivity η . Because the plasma resistivity scales as $T_e^{-3/2}$, for a constant current density the joule heating rate of a plasma decreases as it is heated. Thus, joule heating becomes less effective as the electron temperature increases. Note also that despite the complexity of the dependence of ν_e on T_e , the characteristic time scale for Coulomb collisional relaxation of the electron temperature to its equilibrium value is roughly the same as the ion temperature equilibration time scale τ_{i-e} .

2.5 Numerical Example of Collisional Effects*

In order to illustrate the evaluation of and numerical values for these various collisional processes, we will work them out for a particular plasma example. The plasma example will be chosen to be typical of laboratory experiments for magnetic fusion studies, but the plasma will be assumed to be infinite and uniform, and in equilibrium — so there will not be any spatial or temporal inhomogeneity effects. For the plasma electrons we assume an electron density $n_e = 2 \times 10^{19} \text{ m}^{-3}$ and electron temperature $T_e = 1 \text{ keV}$. For these parameters the electron plasma period [inverse of electron plasma frequency from (??)] is $1/\omega_{pe} = 1/[56(2 \times 10^{19})^{1/2}] \simeq 4 \times 10^{-12} \text{ s}^{-1}$, the electron Debye length from (??) is $\lambda_{De} = 7434 [10^3/(2 \times 10^{19})]^{1/2} \simeq 5.3 \times 10^{-5} \text{ m}$, and the number of electrons in an electron Debye cube is $n_e \lambda_{De}^3 \simeq 3 \times 10^6$. These parameters clearly satisfy the criterion $n_e \lambda_{De}^3 \gg 1$ for the plasma state.

The ions in laboratory plasmas often include impurities in addition to the desired hydrogenic species. We will take into account an impurity species to show how the various plasma collision rates presented in the preceding sections need to be modified to take into account multiple species of ions, and in particular impurities. For our example laboratory plasma we will assume a dominant

deuterium (atomic weight $A_D = 2$, charge $Z_D = 1$) ion species with relative density $n_D/n_e = 0.64$ and fully ionized carbon ($A_C = 12$, $Z_C = 6$) impurities with a relative density of $n_C/n_e = 0.06$. Note that even though the carbon ion density is only 6% of the electron density the carbon ions supply 36% of the ion charge needed for charge neutrality: $\sum_i n_i Z_i = [0.64 + (0.06)(6)]n_e = n_e$. Both the deuterium and carbon ion temperatures will be assumed to be 0.5 keV.

In order to calculate the $\ln \Lambda$ factor for the fundamental electron collision rate we first need to determine the maximum and minimum collisional impact parameters b_{\max} and b_{\min} . The maximum impact parameter is the overall plasma Debye length in the plasma which is defined in (??). For our multi-species plasma the Debye length can be calculated from the electron Debye length by taking out common factors in the ratio of λ_D to λ_{De} :

$$\lambda_D \equiv \lambda_{De} \left[\sum_s \frac{n_s T_e}{n_e T_s} Z_s^2 \right]^{-1/2}, \quad (2.42)$$

which for our plasma yields $\lambda_D = \lambda_{De}/[1 + (0.64)(2) + (0.06)(2)(6^2)]^{1/2} \simeq \lambda_{De}/2.6 \simeq 2 \times 10^{-5}$ m. Classical and quantum mechanical minimum impact parameters for electron-deuteron collisions in this plasma are estimated from (2.9) and (2.10): $b_{\min}^{\text{cl}} = 4.8 \times 10^{-10}/10^3 = 1.4 \times 10^{-12}$ m and $b_{\min}^{\text{qm}} = 1.1 \times 10^{-10}/(10^3)^{1/2} = 3.5 \times 10^{-12}$ m. Since the quantum mechanical impact parameter is larger, we use it for b_{\min} and thus have $\ln \Lambda \equiv \ln(\lambda_D/b_{\min}^{\text{qm}}) \simeq \ln[(2 \times 10^{-5})/(3.5 \times 10^{-12})] \simeq \ln(5.7 \times 10^6) \simeq 16$. Since the Coulomb collision frequency is only accurate to order $1/\ln \Lambda \simeq 1/16 \simeq 0.06$, in the following we will give numerical values to only about 6% accuracy; more accuracy is unwarranted and misleading.

In calculating the electron collision frequency we need to take account of all the ion species. From (2.17) we see that the electron-ion collision frequency is proportional to $n_i Z_i^2$. Thus, for impure plasmas it is convenient to define

$$Z_{\text{eff}} \equiv \frac{\sum_i n_i Z_i^2}{\sum_i n_i Z_i} = \frac{\sum_i n_i Z_i^2}{n_e}, \quad \text{effective ion charge,} \quad (2.43)$$

in which the sum is over all ion species in the plasma. Hereafter in this section we will designate the main ions with a subscript i and the impurities with a subscript Z . For our example plasma we obtain $Z_{\text{eff}} \equiv (n_i Z_i^2 + n_Z Z_Z^2)/n_e = 0.64(1^2) + (0.06)(6^2) = 2.8$. The overall electron collision frequency ν_e defined in (2.17) for an electron-ion plasma can be written for an impure plasma in terms of the electron-deuterium (dominant ion with $Z_i = 1$) collision frequency $\bar{\nu}_S^{e/Z_i=1}$ (in the notation used in Section 2.10) as $\nu_e = Z_{\text{eff}} \bar{\nu}_S^{e/Z_i=1}$, in which

$$\bar{\nu}_S^{e/Z_i=1} \equiv \frac{\nu_e}{Z_{\text{eff}}} = \frac{4\sqrt{2\pi} n_e e^4 \ln \Lambda}{\{4\pi\epsilon_0\}^2 3 m_e^{1/2} T_e^{3/2}} \simeq \frac{5 \times 10^{-11} n_e}{[T_e(\text{eV})]^{3/2}} \left(\frac{\ln \Lambda}{17} \right) \text{ s}^{-1}. \quad (2.44)$$

For our example plasma $\bar{\nu}_S^{e/Z_i=1} \simeq (5 \times 10^{-11})(2 \times 10^{19})(16/17)/(10^3)^{3/2} \simeq 3 \times 10^4 \text{ s}^{-1}$, which gives $\nu_e = (2.8)(3 \times 10^4) \simeq 8.4 \times 10^4$. Hence, for our example

plasma the time scale on which the electron distribution becomes a Maxwellian and electron flows come into equilibrium is $\tau_e \equiv 1/\nu_e \simeq 12 \mu\text{s}$. The distance typical electrons travel in this time is the electron collision length (2.18) $\lambda_e \equiv v_{Te}/\nu_e$, which is about 230 m for our plasma. Finally, the reference electrical resistivity calculated from (2.31) is about $1.5 \times 10^{-7} \Omega \cdot \text{m}$. For impure plasmas it is appropriate to replace the Z_i in (2.33) by Z_{eff} , which then yields $\alpha_e \simeq 0.4$ for $Z_{\text{eff}} \simeq 2.8$. Thus, the Spitzer electrical resistivity for our example plasma is $6 \times 10^{-8} \Omega \cdot \text{m}$. For reference, the resistivity of copper at room temperature is about $1.7 \times 10^{-8} \Omega \cdot \text{m}$, a factor of about 3.5 smaller.

To calculate the ion collision frequency for the dominant ions (subscript i) in an impure plasma we need to include both their self-collisions and their collisions with impurities (subscript Z). Since the masses of impurity ions are rather disparate from the dominant ions ($m_i \ll m_Z \rightarrow A_D \ll A_C$ for our example plasma), the $\sqrt{2}$ rest mass factor is not appropriate for collisions between dominant ions and impurities. Thus, the appropriate collision frequency for the dominant ions in an impure plasma becomes

$$\nu_i = f_i \bar{\nu}_S^{i/i} \quad (2.45)$$

with

$$\bar{\nu}_S^{i/i} \equiv \frac{4\sqrt{\pi} n_i Z_i^4 e^4 \ln \Lambda}{\{4\pi\epsilon_0\}^2 3 m_i^{1/2} T_i^{3/2}} = \left(\frac{n_i Z_i^4}{n_e}\right) \left(\frac{m_e}{m_i}\right)^{1/2} \left(\frac{T_e}{T_i}\right)^{3/2} \frac{\bar{\nu}_S^{e/Z_i=1}}{\sqrt{2}}, \quad (2.46)$$

$$f_i \equiv 1 + \sqrt{2} \left(\frac{n_Z Z_Z^2}{n_i Z_i^2}\right) \left(\frac{m_i}{m_Z}\right)^{1/2}, \quad \text{ion collisions impurity factor.} \quad (2.47)$$

For multiple impurity species (Z) one just sums the second term in f_i over them. For our example plasma $f_i = 1 + \sqrt{2} [(0.06)(6^2)/0.64](2/12)^{1/2} \simeq 3$, and $\nu_i \simeq 3(0.64)(1/3672)^{1/2} 2^{3/2} (3 \times 10^4)/\sqrt{2} \simeq 1.9 \times 10^3 \text{ s}^{-1}$. Thus, the ions will relax toward a Maxwellian distribution and their equilibrium flow on the ion collisional time scale $\tau_i = 1/\nu_i \simeq 530 \mu\text{s}$. The ion collision length defined by $\lambda_i = v_{Ti}/\nu_i$ is about 120 m for our plasma, which is about a factor of two less than the electron collision length λ_e .

Finally, we calculate the longest time scale process — ion-electron energy exchange. We must again take account of impurities in the calculation. Here, since an electron-ion mass ratio is involved, we obtain

$$\bar{\nu}_S^{e/i} = f_{i-e} \left(3 \frac{m_e}{m_i}\right) \left(\frac{n_i Z_i^2}{n_e}\right) \bar{\nu}_S^{e/Z_i=1} \quad (2.48)$$

in which the relevant factor to include impurity effects is

$$f_{i-e} = 1 + \left(\frac{n_Z Z_Z^2}{n_i Z_i^2}\right) \left(\frac{m_i}{m_Z}\right), \quad \text{ion-electron energy exchange impurity factor.} \quad (2.49)$$

Again, for multiple impurity species (Z) one just sums the second term in f_{i-e} over them. For our example plasma $f_{i-e} = 1 + [(0.06)(6^2)/(0.64)](2/12) \simeq$

1.6. In the presence of impurities the time scale for ion-electron temperature equilibration becomes [see discussion after (2.39)] $\tau_{i-e} \equiv 3/(2\bar{\nu}_{\mathcal{E}}^{e/i})$, which for our plasma is $\tau_{i-e} = (3672/2)/[(1.6)(0.64)(3 \times 10^4)] \simeq 60$ ms.

In summary, the electron, ion and ion-electron collision times in our example plasma are $\tau_e : \tau_i : \tau_{i-e} \simeq 12 : 530 : 60\,000 \mu\text{s}$. Their ratios are in rough accord with their anticipated mass ratio scalings of $1 : (m_i/m_e)^{1/2} : m_i/m_e = 1 : 61 : 3672$. Note also that even the electron (shortest) of these collisional time scales are much much longer (by a factor $\sim n_e \lambda_{De}^3 \simeq 3 \times 10^6 \gg 1$) than the plasma oscillation period $1/\omega_{pe} \simeq 4 \times 10^{-6} \mu\text{s}$.

Implicit in the preceding analysis is the assumption that no other physical processes operate on the charged particles in the plasma on these characteristic collision time ($\simeq \tau_e - \tau_{i-e} \sim 10 - 10^4 \mu\text{s}$) or length ($\simeq \lambda_e, \lambda_i \gtrsim 100$ m) scales. In practice, in most plasmas many other processes (for example, temporal variations, gyromotion in magnetic fields, and spatial inhomogeneities) vary more rapidly than one or more of these collisional effects and modify or impede the collisional processes. Such combined collision and geometric effects will be discussed later, particularly in Part IV: Transport. Note, however, that even in the limit of very short time scales (compared to τ_e) Coulomb collision effects are not insignificant; as indicated by (2.20), in a time t they diffusively spread the velocity vectors of charged particles in a plasma through a pitch-angle $\vartheta \simeq v_{\perp}/v \simeq (\nu t)^{1/2}$. This velocity diffusion effect is important in smoothing out sharp gradients in velocity space and leads to collisional boundary layers in otherwise “collisionless” plasmas. Thus, Coulomb collisions will often play a significant role even in “collisionless” plasmas. In fact, as we will see in later chapters, Coulomb collisions provide the fundamental irreversibility (entropy-producing dissipative mechanisms) in plasmas.

2.6 Collisions with a Moving Background+

The most general Coulomb collision processes are those where a test particle species (s) collides with an arbitrary background species (s') of plasma particles that are in motion, which we now consider. The test particle charge, mass, position and velocity vectors will be taken to be q_s, m_s, \mathbf{x} and \mathbf{v} while the corresponding quantities for the background particles will be indicated by the corresponding primed quantities: $q_{s'}, m_{s'}, \mathbf{x}'$ and \mathbf{v}' . The background particles will be assumed to have an arbitrary velocity distribution given by $f_{s'}(\mathbf{v}')$.

The procedure we follow to determine the Coulomb collision processes for this general case follows that used in the Lorentz collision model except that now the basic interaction is most conveniently calculated in a center-of-mass (or really -momentum) frame. To develop the equations of motion in a center-of-momentum frame, we first note that the equations of motion of the interacting test and background particles are given by

$$m_s \frac{d\mathbf{v}}{dt} = q_s \mathbf{E}(\mathbf{x}) = \frac{q_s q_{s'}}{\{4\pi\epsilon_0\}} \frac{\mathbf{x} - \mathbf{x}'}{|\mathbf{x} - \mathbf{x}'|^3}, \quad (2.50)$$

$$m_{s'} \frac{d\mathbf{v}'}{dt} = q_{s'} \mathbf{E}(\mathbf{x}') = \frac{q_s q_{s'}}{\{4\pi\epsilon_0\}} \frac{\mathbf{x}' - \mathbf{x}}{|\mathbf{x}' - \mathbf{x}|^3}. \quad (2.51)$$

Note that the forces in these equations are equal and opposite — because of the conservative nature of the Coulomb force. Defining the center-of-momentum position \mathbf{R} and velocity \mathbf{U} vectors as

$$\mathbf{R} = \frac{m_s \mathbf{x} + m_{s'} \mathbf{x}'}{m_s + m_{s'}}, \quad \mathbf{U} = \frac{m_s \mathbf{v} + m_{s'} \mathbf{v}'}{m_s + m_{s'}}, \quad (2.52)$$

and the corresponding relative position \mathbf{r} and velocity \mathbf{u} vectors

$$\mathbf{r} = \mathbf{x} - \mathbf{x}', \quad \mathbf{u} = \mathbf{v} - \mathbf{v}', \quad (2.53)$$

we find the equations of motion in (2.50), (2.51) become

$$\frac{d\mathbf{U}}{dt} = \mathbf{0}, \quad m_{ss'} \frac{d\mathbf{u}}{dt} = \frac{q_s q_{s'} \mathbf{r}}{\{4\pi\epsilon_0\} |\mathbf{r}|^3}, \quad (2.54)$$

in which $m_{ss'}$ is defined by

$$\boxed{m_{ss'} \equiv \frac{m_s m_{s'}}{m_s + m_{s'}}, \quad \text{reduced mass.}} \quad (2.55)$$

From the first relation in (2.54) we see that the center-of-momentum velocity \mathbf{U} is constant throughout the collisional interaction of the particles.

The equation describing the force on the relative velocity $\mathbf{u} \equiv \mathbf{v} - \mathbf{v}'$ in (2.54) is analogous to that in (2.2) for the Lorentz collision model. Adopting a coordinate system analogous to that in Fig. 2.3 in which v is replaced by $u \equiv |\mathbf{v} - \mathbf{v}'|$, we readily find that the change $\Delta \mathbf{u}$ in a single Coulomb collision interaction between a test particle (s) and background particle (s') is

$$\Delta \mathbf{u}_\perp = \frac{1}{m_{ss'}} \int_{-\infty}^{\infty} dt \frac{q_s q_{s'} \mathbf{r}}{\{4\pi\epsilon_0\} r^3} = \frac{2q_s q_{s'}}{\{4\pi\epsilon_0\} m_{ss'} b u} (\hat{\mathbf{e}}_x \cos \varphi + \hat{\mathbf{e}}_y \sin \varphi). \quad (2.56)$$

Since the total energy is constant in the center-of-momentum frame for an elastic Coulomb collision, using a geometry analogous to that in Fig. 2.4, with \mathbf{v} replaced by the relative velocity \mathbf{u} , and relations (2.5), (2.6), we obtain

$$\mathbf{u} \cdot \Delta \mathbf{u} = -\frac{1}{2} \Delta \mathbf{u} \cdot \Delta \mathbf{u} \simeq -\frac{1}{2} \Delta \mathbf{u}_\perp \cdot \Delta \mathbf{u}_\perp \implies \Delta u_\parallel = -\frac{2q_s^2 q_{s'}^2}{\{4\pi\epsilon_0\}^2 m_{ss'}^2 b^2 u^3}. \quad (2.57)$$

Next, we want to determine the dynamical friction and diffusion coefficients $\langle \Delta \mathbf{v} \rangle^{s/s'}$ and $\langle \Delta \mathbf{v} \Delta \mathbf{v} \rangle^{s/s'}$ for test particles s colliding with background particles s' . To do so we must relate $\Delta \mathbf{v}$ to the relative $\Delta \mathbf{u}$ determined above. Utilizing the momentum conservation relations arising from $\mathbf{U} = \text{constant}$ in (2.52) with $\mathbf{v} \rightarrow \mathbf{v} + \Delta \mathbf{v}$, $\mathbf{v}' \rightarrow \mathbf{v}' + \Delta \mathbf{v}'$ and $\mathbf{u} \rightarrow \mathbf{u} + \Delta \mathbf{u}$ from before to after the collision, we find

$$\Delta \mathbf{v}' = -\frac{m_s}{m_{s'}} \Delta \mathbf{v}, \quad \Delta \mathbf{v} = \frac{m_{ss'}}{m_s} \Delta \mathbf{u}. \quad (2.58)$$

Then, taking account of the velocity distribution $f_{s'}(\mathbf{v}')$ of the background particles, we define the average vectorial dynamical friction and tensorial velocity diffusion coefficients to be

$$\frac{\langle \Delta \mathbf{v} \rangle^{s/s'}}{\Delta t} \equiv \int d^3v' f_{s'}(\mathbf{v}') u \int d\varphi \int b db \frac{m_{ss'}}{m_s} \Delta \mathbf{u}, \quad (2.59)$$

$$\frac{\langle \Delta \mathbf{v} \Delta \mathbf{v} \rangle^{s/s'}}{\Delta t} \equiv \int d^3v' f_{s'}(\mathbf{v}') u \int d\varphi \int b db \frac{m_{ss'}^2}{m_s^2} \Delta \mathbf{u} \Delta \mathbf{u}. \quad (2.60)$$

Using (2.56) and (2.57), the integrations in (2.59) and (2.60) can be performed with a specification of the impact parameter integral in (2.11) generalized to a test particle (s) colliding with a moving background (s') as follows:

$$\ln \Lambda_{ss'} \equiv \int_{b_{\min}}^{b_{\max}} \frac{db}{b} = \ln \left(\frac{\lambda_D}{b_{\min}} \right), \quad b_{\min} = \max \{ b_{\min}^{\text{cl}}, b_{\min}^{\text{qm}} \} \quad (2.61)$$

in which

$$b_{\min}^{\text{cl}} \equiv \frac{q_s q_{s'}}{\{4\pi\epsilon_0\} m_{ss'} \overline{u^2}}, \quad b_{\min}^{\text{qm}} = \frac{h}{4\pi m_{ss'} \sqrt{\overline{u^2}}}. \quad (2.62)$$

The $\overline{u^2}$ indicates an average of u^2 over the distribution of background particles; an appropriate typical value for this quantity is given in (2.113) below. In what follows we will implicitly assume that $\ln \Lambda_{ss'}$ is independent of \mathbf{v}' so that it can be brought outside the \mathbf{v}' integration in equations (2.59) and (2.60); retaining the $\ln \Lambda$ inside the \mathbf{v}' integration would only yield negligible (additional) corrections of order $1/\ln \Lambda$ to the results we obtain below.

Thus, performing the integrations in (2.59) and (2.60) utilizing the impact parameter integral in (2.61) and the facts that

$$\frac{\partial u}{\partial \mathbf{v}} = \frac{\mathbf{u}}{u}, \quad \frac{\partial}{\partial \mathbf{v}} \frac{1}{u} = -\frac{\mathbf{u}}{u^3}, \quad \frac{\partial^2 u}{\partial \mathbf{v} \partial \mathbf{v}} = \frac{u^2 \mathbf{I} - \mathbf{u} \mathbf{u}}{u^3} = \frac{1}{u} (\hat{\mathbf{e}}_x \hat{\mathbf{e}}_x + \hat{\mathbf{e}}_y \hat{\mathbf{e}}_y), \quad (2.63)$$

for our present velocity space coordinate system we obtain (for an alternate derivation using the Rutherford differential scattering cross section see Problem 2.24):

$$\frac{\langle \Delta \mathbf{v} \rangle^{s/s'}}{\Delta t} = -\frac{m_s}{m_{ss'}} \Gamma_{ss'} \int d^3v' f_{s'}(\mathbf{v}') \frac{\mathbf{u}}{u^3} \equiv \Gamma_{ss'} \frac{\partial H_{s'}(\mathbf{v})}{\partial \mathbf{v}}, \quad (2.64)$$

$$\frac{\langle \Delta \mathbf{v} \Delta \mathbf{v} \rangle^{s/s'}}{\Delta t} = \Gamma_{ss'} \int d^3v' f_{s'}(\mathbf{v}') \frac{u^2 \mathbf{I} - \mathbf{u} \mathbf{u}}{u^3} \equiv \Gamma_{ss'} \frac{\partial^2 G_{s'}(\mathbf{v})}{\partial \mathbf{v} \partial \mathbf{v}}, \quad (2.65)$$

in which

$$\Gamma_{ss'} \equiv \frac{4\pi q_s^2 q_{s'}^2 \ln \Lambda_{ss'}}{\{4\pi\epsilon_0\}^2 m_s^2}, \quad (2.66)$$

$$G_{s'}(\mathbf{v}) \equiv \int d^3v' f_{s'}(\mathbf{v}') |\mathbf{v} - \mathbf{v}'|, \quad (2.67)$$

$$H_{s'}(\mathbf{v}) \equiv \frac{m_s}{m_{ss'}} \int d^3v' \frac{f_{s'}(\mathbf{v}')}{|\mathbf{v} - \mathbf{v}'|} = \left(1 + \frac{m_s}{m_{s'}} \right) \int d^3v' \frac{f_{s'}(\mathbf{v}')}{|\mathbf{v} - \mathbf{v}'|}. \quad (2.68)$$

The G and H functions are formally similar to the electrostatic potential due to a distributed charge density for which Poisson's equation $-\nabla^2\phi = \rho_q(\mathbf{x})/\epsilon_0$ has the solution $\phi(\mathbf{x}) = \int d^3x' \rho_q(\mathbf{x}')/(\{4\pi\epsilon_0\}|\mathbf{x} - \mathbf{x}'|)$. They are called *Rosenbluth potentials*⁹. Using the facts that

$$\nabla_v^2 \frac{1}{u} \equiv \left(\frac{\partial}{\partial \mathbf{v}} \cdot \frac{\partial}{\partial \mathbf{v}} \right) \frac{1}{u} = -4\pi \delta(\mathbf{u}) = -4\pi \delta(\mathbf{v} - \mathbf{v}'), \quad (2.69)$$

$$\nabla_v^2 u = \frac{\partial}{\partial \mathbf{v}} \cdot \frac{\partial u}{\partial \mathbf{v}} = \frac{\partial}{\partial \mathbf{v}} \cdot \left(\frac{\mathbf{u}}{u} \right) = \frac{2}{u}, \quad (2.70)$$

the Rosenbluth potentials can be shown to satisfy the relations

$$\begin{aligned} \nabla_v^2 H_{s'}(\mathbf{v}) &= -4\pi (1 + m_s/m_{s'}) f_{s'}(\mathbf{v}), \\ \nabla_v^2 G_{s'}(\mathbf{v}) &= 2 H_{s'}(\mathbf{v}) / (1 + m_s/m_{s'}), \\ \nabla_v^2 \nabla_v^2 G_{s'}(\mathbf{v}) &= -8\pi f_{s'}(\mathbf{v}). \end{aligned} \quad (2.71)$$

Note that since the second of these equations shows that $H_{s'}$ is proportional to a Laplacian velocity space derivative of $G_{s'}$, the Rosenbluth potential $G_{s'}$ is the fundamental one from which all needed quantities can be derived.

From the analogy of the first of the forms in (2.71) to electrostatics and the definition of $\langle \Delta \mathbf{v} \rangle / \Delta t$ in (2.64) in terms of the Rosenbluth potential $H_{s'}$, we see that the dynamical friction $\langle \Delta \mathbf{v} \rangle / \Delta t$ tries to relax the test particle velocity to the centroid of the velocity distribution of the background particles $f_{s'}(\mathbf{v})$ — see Problems 2.25 and 2.26. However, the velocity space diffusion $\langle \Delta \mathbf{v} \Delta \mathbf{v} \rangle / \Delta t$ causes the velocity distribution of the test particles to maintain a thermal spread comparable to that of the background particles. The dynamical balance between these two collisional processes on an entire distribution of test particles determines their collisional distribution function — see Chapter 11.

Finally, using (2.63) and vector identities from Appendix D.3, we note that

$$\frac{\partial}{\partial \mathbf{v}} \cdot \left(\frac{u^2 \mathbf{I} - \mathbf{u} \mathbf{u}}{u^3} \right) = \left(\frac{\partial}{\partial \mathbf{v}} \frac{1}{u} \right) \cdot \mathbf{I} - \left(\frac{\partial}{\partial \mathbf{v}} \frac{1}{u^3} \right) \cdot \mathbf{u} \mathbf{u} - \frac{1}{u^3} \frac{\partial}{\partial \mathbf{v}} \cdot \mathbf{u} \mathbf{u} = -2 \frac{\mathbf{u}}{u}. \quad (2.72)$$

Thus, we find that for Coulomb collisions the dynamical friction and velocity diffusion coefficients are related by the important relation

$$\boxed{\frac{\langle \Delta \mathbf{v} \rangle^{s/s'}}{\Delta t} = \frac{m_s}{2m_{s'}} \frac{\partial}{\partial \mathbf{v}} \cdot \frac{\langle \Delta \mathbf{v} \Delta \mathbf{v} \rangle^{s/s'}}{\Delta t} = \left(\frac{1 + m_s/m_{s'}}{2} \right) \frac{\partial}{\partial \mathbf{v}} \cdot \frac{\langle \Delta \mathbf{v} \Delta \mathbf{v} \rangle^{s/s'}}{\Delta t}.} \quad (2.73)$$

The total collisional effects on a test particle due to Coulomb collisions with all types of background particles are obtained by simply adding the contributions from each species of background particles:

$$\boxed{\frac{\langle \Delta \mathbf{v} \rangle^s}{\Delta t} = \sum_{s'} \frac{\langle \Delta \mathbf{v} \rangle^{s/s'}}{\Delta t}, \quad \frac{\langle \Delta \mathbf{v} \Delta \mathbf{v} \rangle^s}{\Delta t} = \sum_{s'} \frac{\langle \Delta \mathbf{v} \Delta \mathbf{v} \rangle^{s/s'}}{\Delta t}.} \quad (2.74)$$

⁹M.N. Rosenbluth, W. MacDonald and D. Judd, *Phys. Rev.* **107**, 1 (1957).

Note also that the combination of this summation of species effects and, more importantly, of the fact that the Rosenbluth potentials are integrals over the background distribution functions, means that the dynamical friction and velocity diffusion coefficients are not sensitively dependent on detailed features of $f_{s'}(\mathbf{v})$. (Recall the analogous weak dependence of an electrostatic potential to the distribution of charges inside a surface.) Thus, evaluation of the Rosenbluth potentials for Maxwellian background distributions will be useful both in describing test particle collisional processes in Maxwellian plasmas and in other plasmas of interest where the distribution functions are reasonably close to Maxwellians.

2.7 Collisions with a Maxwellian Background+

Specific test particle collisional effects due to dynamical friction and velocity diffusion can be worked out in the rest frame of the background particles for an isotropic Maxwellian velocity distribution of the background particles:

$$f_{Ms'}(\mathbf{v}) = n_{s'} \left(\frac{m_{s'}}{2\pi T_{s'}} \right)^{3/2} e^{-m_{s'} v^2 / 2T_{s'}} = \frac{n_{s'} e^{-v^2 / v_{Ts'}^2}}{\pi^{3/2} v_{Ts'}^3}. \quad (2.75)$$

Here, we have defined a “typical” thermal speed

$$v_{Ts'} \equiv (2T_{s'}/m_{s'})^{1/2}. \quad (2.76)$$

Note that this speed is not the average speed [see (??) in Appendix A.4] for a Maxwellian distribution, which is $(8T_{s'}/\pi m_{s'})^{1/2}$; however, it is the most probable speed [see (??) in Appendix A.4] and it is mathematically convenient.

For a Maxwellian velocity distribution the Rosenbluth potential $G_{s'}(\mathbf{v})$ defined in (2.67) can be evaluated in a spherical coordinate system in the relative velocity space $\mathbf{u} = \mathbf{v} - \mathbf{v}'$ as follows:

$$\begin{aligned} G_{s'}(\mathbf{v}) &\equiv \int d^3v' f_{s'}(\mathbf{v}') |\mathbf{v} - \mathbf{v}'| = \int d^3u f_{s'}(\mathbf{u} + \mathbf{v}) u \\ &= \frac{n_{s'}}{\pi^{3/2} v_{Ts'}^3} \int_0^\infty 2\pi u^2 du \int_{-1}^1 d(\cos \vartheta) u e^{-(v^2 + u^2 + 2uv \cos \vartheta)/v_{Ts'}^2} \\ &= -\frac{n_{s'} v_{Ts'}^2}{\sqrt{\pi} v} \int_0^\infty \frac{u^2 du}{v_{Ts'}^3} \left[e^{-(v+u)^2/v_{Ts'}^2} - e^{-(v-u)^2/v_{Ts'}^2} \right] \\ &= -\frac{n_{s'} v_{Ts'}^2}{\sqrt{x}} \frac{1}{\sqrt{\pi}} \left[-4\sqrt{x} \int_{\sqrt{x}}^\infty dy y e^{-y^2} - 2 \int_0^{\sqrt{x}} dy (y^2 + x) e^{-y^2} \right] \\ &= \frac{n_{s'} v_{Ts'}^2}{\sqrt{x}} \frac{2}{\sqrt{\pi}} \left[2\sqrt{x} \int_{\sqrt{x}}^\infty dy y e^{-y^2} + \int_0^{\sqrt{x}} dy y^2 e^{-y^2} + x \int_0^{\sqrt{x}} dy e^{-y^2} \right] \end{aligned} \quad (2.77)$$

in which $\sqrt{x} \equiv v/v_{Ts'}$. The integrals in the last forms of (2.77) are related to the error function or probability integral (cf., Problem 2.27), but are most

conveniently written in terms of

$$\boxed{\psi(x) \equiv \frac{2}{\sqrt{\pi}} \int_0^x dt \sqrt{t} e^{-t}, \quad \text{Maxwell integral,}} \quad (2.78)$$

which has the properties

$$\psi' \equiv \frac{d\psi}{dx} = \frac{2}{\sqrt{\pi}} \sqrt{x} e^{-x}, \quad \psi + \psi' = \frac{2}{\sqrt{\pi}} \int_0^{\sqrt{x}} dy e^{-y^2} \equiv \text{erf}(\sqrt{x}). \quad (2.79)$$

Physically, the Maxwell integral is the normalized integral of a Maxwellian velocity distribution out to a sphere of radius v . Utilizing these definitions, we find that the Rosenbluth potential $G_{s'}(\mathbf{v})$ for a Maxwellian distribution of background particles can be written as

$$G_{s'}(\mathbf{v}) = n_{s'} v_{Ts'} \frac{1}{\sqrt{x}} [(x+1)\psi'(x) + (x+1/2)\psi(x)], \quad (2.80)$$

in which

$$\boxed{x \equiv x^{s/s'} = \frac{m_{s'} v^2}{2 T_{s'}} = \frac{v^2}{v_{Ts'}^2}, \quad \text{relative speed parameter.}} \quad (2.81)$$

The important parameter $x^{s/s'}$ is the square of the ratio of the test particle speed to the thermal speed of the background particles of species s' .

Thus, for an isotropic Maxwellian velocity distribution of background particles the Rosenbluth potential $G_{s'}(\mathbf{v}) = G_{s'}(v)$; that is, it depends only on the test particle speed v , not its velocity \mathbf{v} . Then, as can be shown from (2.65), $\langle \Delta \mathbf{v} \Delta \mathbf{v} \rangle$ is a diagonal tensor with elements $\langle \Delta v_x^2 \rangle = \langle \Delta v_y^2 \rangle = \langle \Delta v_z^2 \rangle / 2$ and $\langle \Delta v_{\parallel}^2 \rangle$. Further, it can be shown that $\langle \Delta \mathbf{v} \rangle$ is in the $\hat{\mathbf{e}}_z$ or \mathbf{v} direction. [These properties are valid for any distribution function for which the Rosenbluth potential $G_{s'}$ depends only on the test particle speed v .] Substituting the Rosenbluth potential in (2.80) into (2.64) and (2.65), and utilizing (2.71) or (2.73), we find that the relevant dynamical friction and velocity diffusion coefficients are given by

$$\frac{\langle \Delta v_{\parallel} \rangle^{s/s'}}{\Delta t} = \Gamma_{ss'} \frac{m_s}{2m_{s'}} \frac{\partial}{\partial v} \left[\frac{1}{v^2} \frac{\partial}{\partial v} \left(v^2 \frac{\partial G_{s'}}{\partial v} \right) \right] = - \left[\frac{m_s}{m_{s'}} \psi(x) \right] \nu_0^{s/s'} v, \quad (2.82)$$

$$\frac{\langle \Delta v_{\perp}^2 \rangle^{s/s'}}{\Delta t} = \Gamma_{ss'} \frac{2}{v} \frac{\partial G_{s'}}{\partial v} = 2 \left[\psi(x) \left(1 - \frac{1}{2x} \right) + \psi'(x) \right] \nu_0^{s/s'} v^2, \quad (2.83)$$

$$\frac{\langle \Delta v_{\parallel}^2 \rangle^{s/s'}}{\Delta t} = \Gamma_{ss'} \frac{\partial^2 G_{s'}}{\partial v^2} = \left[\frac{\psi(x)}{x} \right] \nu_0^{s/s'} v^2. \quad (2.84)$$

Note that in contrast to the Lorentz collision model, we now find $\langle \Delta v_{\parallel}^2 \rangle \neq 0$ — because the background particles are of finite mass and in motion, and hence can exchange energy with the test particle during a Coulomb collision. The net rate of change of the test particle energy, which is given by $(m/2) \langle \Delta v^2 \rangle / \Delta t \equiv$

$(m/2)\langle(\mathbf{v} + \Delta\mathbf{v}) \cdot (\mathbf{v} + \Delta\mathbf{v}) - v^2\rangle/\Delta t$, can be determined from these coefficients as well:

$$\begin{aligned}\frac{\langle\Delta v^2\rangle^{s/s'}}{\Delta t} &= 2v \frac{\langle\Delta v_{\parallel}\rangle^{s/s'}}{\Delta t} + \frac{\langle\Delta v_{\perp}^2\rangle^{s/s'}}{\Delta t} + \frac{\langle\Delta v_{\parallel}^2\rangle^{s/s'}}{\Delta t} \\ &= -2[(m_s/m_{s'})\psi(x) - \psi'(x)]\nu_0^{s/s'}v^2.\end{aligned}\quad (2.85)$$

The fundamental collision frequency for all these processes is

$$\begin{aligned}\nu_0^{s/s'}(v) &\equiv \frac{n_{s'}\Gamma_{ss'}}{v^3} = \frac{4\pi n_{s'}q_s^2q_{s'}^2}{\{4\pi\epsilon_0\}^2m_s^2v^3} \ln \Lambda_{ss'}, \quad \text{reference collision frequency,} \\ &\simeq (6.6 \times 10^{-11} \text{s}^{-1}) \frac{n_{s'}Z_s^2Z_{s'}^2}{(m_s/m_e)^{1/2}(E_s/\text{eV})^{3/2}} \left(\frac{\ln \Lambda_{ss'}}{17}\right),\end{aligned}\quad (2.86)$$

which is a straightforward generalization of the collision frequency $\nu(v)$ derived for the Lorentz collision model in (2.14): $\nu_0^{e/i} = \nu(v) = \nu_e(3\sqrt{\pi}/4)v_{Te}^3/v^3$.

These dynamical friction and velocity diffusion coefficients can be used to elucidate the rates at which the various Coulomb collision processes affect the test particle velocity. Thus, we define the rates for momentum loss or slowing down (ν_S), perpendicular diffusion (ν_{\perp}), parallel or speed diffusion (ν_{\parallel}) and energy loss (ν_{ε}) resulting from collisions of a test particle s on a Maxwellian velocity distribution of background particles s' as follows:¹⁰

$$\begin{aligned}\frac{d}{dt}(m_s\mathbf{v}) &= -\nu_S^{s/s'}m_s\mathbf{v} \equiv m_s \frac{\langle\Delta\mathbf{v}\rangle^{s/s'}}{\Delta t}, \quad \text{momentum loss,} \\ \frac{d}{dt}|\mathbf{v} - \bar{\mathbf{v}}|_{\perp}^2 &= \nu_{\perp}^{s/s'}v^2 \equiv \frac{\langle\Delta v_{\perp}^2\rangle^{s/s'}}{\Delta t}, \quad \text{perpendicular diffusion,} \\ \frac{d}{dt}|\mathbf{v} - \bar{\mathbf{v}}|_{\parallel}^2 &= \nu_{\parallel}^{s/s'}v^2 \equiv \frac{\langle\Delta v_{\parallel}^2\rangle^{s/s'}}{\Delta t}, \quad \text{parallel diffusion,} \\ \frac{d}{dt}\varepsilon_s &= -\nu_{\varepsilon}^{s/s'}\varepsilon_s \equiv \frac{m_s}{2} \frac{\langle\Delta v^2\rangle^{s/s'}}{\Delta t}, \quad \text{energy loss.}\end{aligned}\quad (2.87)$$

Here, $m_s\mathbf{v}$ is the test particle momentum, $\bar{\mathbf{v}}$ is its average velocity [see (2.97) and (2.104) below for a detailed specification of $\bar{\mathbf{v}}$], $|\mathbf{v} - \bar{\mathbf{v}}|_{\perp}^2$ and $|\mathbf{v} - \bar{\mathbf{v}}|_{\parallel}^2$ indicate the diffusional spread of the test particle velocity in directions perpendicular and parallel to its direction of motion, and $\varepsilon_s \equiv m_sv^2/2$ is the test particle energy.

From the definitions in (2.85) through (2.87) we see that ν_{ε} is not an independent quantity:

$$\nu_{\varepsilon} = 2\nu_S - \nu_{\perp} - \nu_{\parallel}.\quad (2.88)$$

¹⁰For an alternative representation of these various collisional processes using the notation and functions Chandrasekhar introduced for stellar collisions see Problem 2.27.

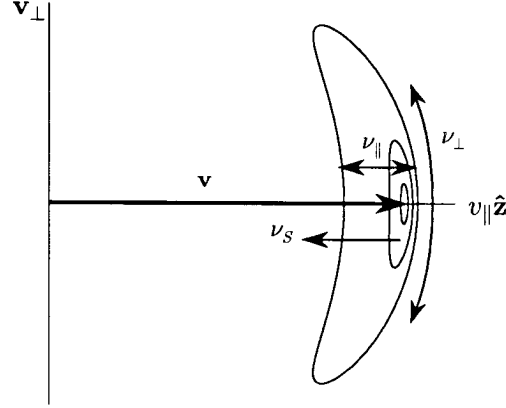


Figure 2.7: Coulomb collisional effects on the velocity of a test particle: momentum loss or slowing down (ν_S), angular or perpendicular (ν_\perp) and speed or parallel (ν_\parallel) diffusion of the original test particle velocity. The contours shown are lines of $e^{-1} \simeq 0.37$ probability (see Section 2.10) at the short times $(t_1, t_2, t_3) = (0.002, 0.02, 0.2)/\nu_\perp$ for an energetic electron ($m_e v^2/2T_e = 10$) in an electron-proton plasma for which $\nu_\parallel/\nu_\perp \simeq 1/40$, $\nu_S/\nu_\perp \simeq 1/2$.

From (2.82)–(2.88), we find the relevant frequencies for collisions of a test particle (species s) with a Maxwellian background (species s') are

$$\nu_S^{s/s'} = - \left[\left(1 + \frac{m_s}{m_{s'}} \right) \psi \right] \nu_0^{s/s'}, \quad \text{momentum loss, slowing down} \quad (2.89)$$

$$\nu_\perp^{s/s'} = 2 \left[\psi + \psi' - \frac{\psi}{2x} \right] \nu_0^{s/s'}, \quad \text{perpendicular, pitch-angle diffusion,} \quad (2.90)$$

$$\nu_\parallel^{s/s'} = \left[\frac{\psi}{x} \right] \nu_0^{s/s'}, \quad \text{parallel, speed diffusion,} \quad (2.91)$$

$$\nu_\varepsilon^{s/s'} = 2 \left[\frac{m_s}{m_{s'}} \psi - \psi' \right] \nu_0^{s/s'} = 2 \nu_S^{s/s'} - \nu_\perp^{s/s'} - \nu_\parallel^{s/s'}, \quad \text{energy loss.} \quad (2.92)$$

The total effects due to a test particle's collisions with all species of background particles are obtained by summing over s' as indicated in (2.74); for example, $\nu_S^s \equiv \sum_{s'} \nu_S^{s/s'}$. The overall effects of Coulomb collisions in slowing down and diffusing the test particle velocity are indicated schematically in Fig. 2.7.

Equations (2.81)–(2.92) provide a very complete and useful description of the evolution of the velocity of a test particle of species s suffering Coulomb collisions with Maxwellian background particles s' — see Problems 2.28–2.33

for some illustrative applications of them. In addition, as discussed in the next section, they can be used to develop a Monte Carlo scattering operator for numerical studies of the effects of Coulomb collisions on the velocity of a test particle. Finally, as we did for the Lorentz collision model [cf., (2.22), (2.23)], we write the dynamical friction and velocity diffusion coefficients for Coulomb collisions of test particles of species s with a species s' of Maxwellian background particles in coordinate-independent vectorial forms:

$$\boxed{\frac{\langle \Delta \mathbf{v} \rangle^{s/s'}}{\Delta t} = -\nu_S^{s/s'} \mathbf{v}, \quad \text{dynamical friction,}} \quad (2.93)$$

$$\boxed{\frac{\langle \Delta \mathbf{v} \Delta \mathbf{v} \rangle^{s/s'}}{\Delta t} = \frac{1}{2} \nu_{\perp}^{s/s'} (v^2 \mathbf{I} - \mathbf{v} \mathbf{v}) + \nu_{\parallel}^{s/s'} \mathbf{v} \mathbf{v}, \quad \text{velocity diffusion.}} \quad (2.94)$$

2.8 Evolution of Test Particle Velocity+

To further illustrate the Coulomb collision effects, we examine the collisional evolution of the velocity of a test particle for short times where the velocity changes are small. The test particle will be assumed to be colliding with a plasma whose components have Maxwellian distributions. Thus, the results of the previous section will be applicable.

A test particle of species s will be taken to have an initial velocity \mathbf{v}_0 in the $\hat{\mathbf{e}}_z$ or parallel direction (cf., Figs. 2.4 and 2.7). Integrating the first equation of (2.87) over a short time $t \gg \Delta t$ (for validity of the dynamical friction and velocity diffusion coefficients), we find that the mean parallel or $\hat{\mathbf{e}}_z$ component of the test particle velocity after a time t is

$$\overline{v_{\parallel}} = v_0(1 - \nu_S t), \quad \nu_S = \nu_S^s \equiv \sum_{s'} \nu_S^{s/s'}(v_0). \quad (2.95)$$

This result is valid for $\nu_S t \ll 1$ and indicates the monotonic decrease in test particle momentum due to Coulomb collisions. Similarly, the test particle energy after a short time t can be obtained directly by integrating the last equation of (2.87) over time:

$$\frac{1}{2} m \overline{v^2} = \frac{1}{2} m v_0^2 (1 - \nu_{\varepsilon} t), \quad \nu_{\varepsilon} = \nu_{\varepsilon}^s \equiv \sum_{s'} \nu_{\varepsilon}^{s/s'}(v_0). \quad (2.96)$$

Thus, the average test particle speed \overline{v} , which will be used below, is defined by

$$\overline{v} \equiv \sqrt{\overline{v^2}} \simeq v_0(1 - \nu_{\varepsilon} t/2). \quad (2.97)$$

Similar to (2.95), these formulas are only valid for $\nu_{\varepsilon} t \ll 1$.

The angular (perpendicular) velocity and speed (parallel) diffusion processes in velocity space indicated by ν_{\perp} and ν_{\parallel} have to be treated differently. Because these Coulomb collision effects are random in character and diffusive, they lead to a Gaussian probability distribution $P(\mathbf{v} - \overline{\mathbf{v}})$ of the velocity about the average

(slowing down) test particle speed \bar{v} . Since the diffusion results from purely random processes, we can anticipate (and will derive in Chapter 11) that this probability distribution will be Gaussian and of the form:

$$P(\mathbf{v} - \bar{\mathbf{v}}) = \frac{1}{2\pi \bar{v}^2} \left(\frac{e^{-\vartheta^2/2\sigma_\perp^2}}{\sigma_\perp^2} \right) \left(\frac{e^{-(v-\bar{v})^2/2\sigma_\parallel^2}}{\sqrt{2\pi} \sigma_\parallel} \right). \quad (2.98)$$

Here, $\vartheta^2 \equiv [\arcsin^{-1}(v_\perp/v_0)]^2 \simeq (v_x^2 + v_y^2)/v_0^2$ and \bar{v} is defined in (2.97). Note that since in the limit $\sigma_\parallel \rightarrow 0$ the last term in braces becomes $\delta(v - \bar{v})$ [see (??) and (??) in Appendix B.2], this probability distribution reduces to the short time Lorentz model test particle distribution given in (2.21) for $\sigma_\perp = \sqrt{\nu t}$.

Taking velocity-space averages of various quantities $A(\mathbf{v})$ over this probability distribution [$\bar{A} \equiv \int_0^\infty 2\pi v^2 dv \int_0^\pi \sin \vartheta d\vartheta P(\mathbf{v} - \bar{\mathbf{v}}) A(\mathbf{v})$], we find that while the average of the diffusive deflections vanish [$\bar{v}_x = \bar{v}_y = 0, \bar{v}_\parallel - \bar{v}_\parallel = 0$], the diffusive spreads in the perpendicular and parallel (to \mathbf{v}_0) directions are

$$\overline{v^2} - \bar{v}^2 \simeq \overline{v_\perp^2} = \overline{v_x^2} + \overline{v_y^2} = 2\sigma_\perp^2 v_0^2, \quad \overline{(v_\parallel - \bar{v}_\parallel)^2} = \sigma_\parallel^2. \quad (2.99)$$

To determine the probability variances σ_\perp and σ_\parallel for the diffusive Coulomb collisional processes, we integrate the middle two equations in (2.87) over a short time t , and obtain (keeping only first order terms in $\nu t \ll 1$)

$$\overline{v_\perp^2} = (\nu_\perp t) v_0^2, \quad \nu_\perp = \nu_\perp^s \equiv \sum_{s'} \nu_\perp^{s/s'}(v_0), \quad (2.100)$$

$$\overline{(v_\parallel - \bar{v}_\parallel)^2} = (\nu_\parallel t) v_0^2, \quad \nu_\parallel = \nu_\parallel^s \equiv \sum_{s'} \nu_\parallel^{s/s'}(v_0). \quad (2.101)$$

Comparing (2.99), (2.100) and (2.101), we see that for Coulomb collisions

$$\sigma_\perp = \sqrt{\nu_\perp t/2}, \quad \sigma_\parallel = \sqrt{\nu_\parallel t} v_0. \quad (2.102)$$

The relative collisional spreads (half-widths in velocity space to points where the probability distribution drops to $e^{-1/2} \simeq 0.61$ of its peak value) of the test particle velocity in the directions perpendicular and parallel (i.e., for speed or energy diffusion) relative to its initial velocity \mathbf{v}_0 are given by

$$\delta\vartheta \simeq \delta v_\perp/v_0 \equiv \sigma_\perp = \sqrt{\nu_\perp t/2}, \quad \delta v/v_0 \equiv \sigma_\parallel/v_0 = \sqrt{\nu_\parallel t}. \quad (2.103)$$

Note that in comparing the perpendicular diffusion factor in (2.98) for which $\sigma_\perp = \sqrt{\nu_\perp t/2}$ with the perpendicular diffusion in the Lorentz model as given in (2.21), we need to realize that $\nu_\perp = 2\nu$ and hence that $\sigma_\perp = \sqrt{\nu t}$ for the Lorentz collision model. These formulas indicate that, even for very high temperature plasmas with $n\lambda_D^3 \gg 1$ where the Coulomb collision rates are very slow, only a short time is required to diffuse the test particle velocity through a small $|\delta\mathbf{v}| \ll |\mathbf{v}_0|$. For example, as indicated in (2.20), the time required to diffuse a particle's velocity through a small angle $\vartheta \simeq \delta v_\perp/v_0 \ll 1$ is only $t \simeq 2\vartheta^2/\nu_\perp \ll 1/\nu_\perp$ [or, $t \simeq \vartheta^2/\nu \ll 1/\nu$ for the Lorentz collision model]. Thus, because of the

diffusive nature of Coulomb collisions, it takes much less time to scatter through an angle $\vartheta \ll 1$ in velocity space than it does to scatter through 90° ($\vartheta \sim 1$). The various diffusive collisional effects are illustrated in Fig. 2.7. There, the contours shown indicate where the probability distribution P in (2.98) is equal to $e^{-1} \simeq 0.37$ of its peak value for $\nu_\perp t = 0.002, 0.02, 0.2$, for a typical set of test particle parameters.

The change in the average energy $mv^2/2$ can also be obtained using (2.95), (2.99) and (2.102). This procedure yields, correct to first order in $\nu t \ll 1$,

$$\begin{aligned} \frac{1}{2}mv^2 &= \frac{1}{2}m \left[\overline{v_\parallel^2} + \overline{v_\perp^2} \right] = \frac{1}{2}m \left[\overline{v_\parallel^2} + 2\overline{(v_\parallel - \overline{v_\parallel})v_\parallel} + \overline{(v_\parallel - \overline{v_\parallel})^2} + \overline{v_\perp^2} \right] \\ &\simeq \frac{1}{2}m[v_0^2(1 - 2\nu_S t) + \sigma_\parallel^2 + 2\sigma_\perp^2] = \frac{1}{2}mv_0^2[1 - (2\nu_S - \nu_\perp - \nu_\parallel)t]. \end{aligned}$$

This result is the same as (2.96) because of the relation between the various collisional processes given in (2.88).

The formulas developed in this section also provide a basis for a probabilistic (Monte Carlo) numerical approach for inclusion of Coulomb collision effects in other plasma processes such as single particle trajectories. Thus far we have found that after a short time t a test particle's velocity and speed decrease according to (2.95) and (2.97). However, the test particle also acquires a diffusive spread in the perpendicular and parallel directions as given by (2.98) with the spreads (variances) defined in (2.102). Further, the velocity space latitudinal angle φ [cf., (2.1)] is completely randomized by successive individual Coulomb collisions — for time scales $t \gg \Delta t$. Hence, defining a random variable ξ to be evenly distributed between 0 and 1, and independent random variables η_1, η_2 sampled from a normal probability distribution [i.e., Gaussian such as indicated in the σ_\parallel part of (2.98)] with zero mean and a mean square of unity (i.e., $\overline{\eta_1} = \overline{\eta_2} = 0$ but $\overline{\eta_1^2} = \overline{\eta_2^2} = 1$), we find that the total velocity vector \mathbf{v} after a short time t ($\nu t \ll 1$) can be written as

$$\mathbf{v} = v_0(1 - \nu_\varepsilon t/2) \left[\hat{\mathbf{e}}_z(1 + \eta_1\sqrt{\nu_\parallel t}) + |\eta_2|\sqrt{\nu_\perp t/2}(\hat{\mathbf{e}}_x \cos 2\pi\xi + \hat{\mathbf{e}}_y \sin 2\pi\xi) \right]. \quad (2.104)$$

In the Lorentz collision model where $\nu_\varepsilon = 0$ and $\nu_\parallel = 0$, this result simplifies to

$$\mathbf{v} = v_0 \left[\hat{\mathbf{e}}_z + |\eta_2|\sqrt{\nu_\perp t/2}(\hat{\mathbf{e}}_x \cos 2\pi\xi + \hat{\mathbf{e}}_y \sin 2\pi\xi) \right], \quad \text{Lorentz collision model.} \quad (2.105)$$

Either of these forms can be used to develop a Monte Carlo algorithm for advancing the test particle velocity \mathbf{v} taking into account the Coulomb collision dynamical friction and velocity space diffusion effects.

Since (2.104) implies a change in the velocity of the test particle, in order to preserve the momentum and energy conserving properties of the elastic Coulomb collision process, the velocity of the background particles must also change, at least on average. Hence, in order to develop a complete Monte Carlo-based Coulomb collision operator we should consider simultaneously both a test

and a background particle. Then, the change in velocity $\delta\mathbf{v} \equiv \mathbf{v} - \mathbf{v}_0$ for the test particle is determined from (2.104), and that for the background particle is given by $\delta\mathbf{v}' = -(m_s/m_{s'})\delta\mathbf{v}$ — see (2.58).

2.9 Test Particle Collision Rates+

We now consider the various Coulomb collision effects on typical electrons and ions in a plasma. For simplicity the plasma will be assumed to be composed of electrons and only one species of ions with charge $q_i = Z_i e$, and to have equal electron and ion temperatures, with both species of particles having Maxwellian velocity distributions. Thus, the formulas derived in the Section 2.7 will apply.

For illustrative purposes we consider collisional effects on a test electron and a test ion in the plasma, each having speeds equal to the thermal or most probable speeds for their respective species:

$$v_e = v_{Te}, \quad v_i = v_{Ti}. \quad (2.106)$$

Then, the reference collision frequencies $\nu_0^{s/s'}$ for electron-ion (e/i), electron-electron (e/e), ion-ion (i/i) and ion-electron (i/e) collisions are simply related:

$$\nu_0^{e/i} = Z_i \nu_0^{e/e}, \quad \nu_0^{i/i} = Z_i^2 \sqrt{m_e/m_i} \nu_0^{e/i}, \quad \nu_0^{i/e} = Z_i \sqrt{m_e/m_i} \nu_0^{e/i}, \quad (2.107)$$

in which we have neglected the small differences in $\ln \Lambda_{ss'}$ for differing s and s' and made use of the quasineutrality condition $n_e = n_i Z_i$. Further, since the ratio of ion to electron mass is very large (1836 for protons), we find that the relative speed parameters $x^{s/s'}$ defined in (2.81) for the various collisional processes are given by

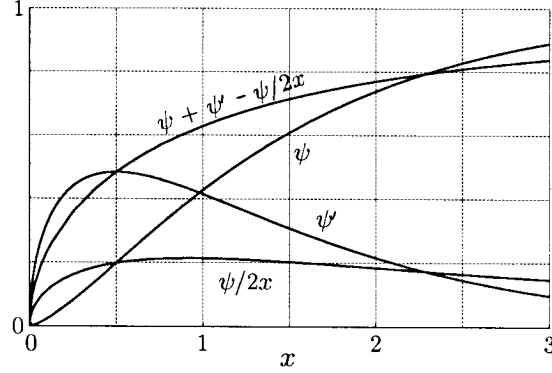
$$x^{e/i} = \frac{m_i}{m_e} \gg 1, \quad x^{e/e} = 1, \quad x^{i/i} = 1, \quad x^{i/e} = \frac{m_e}{m_i} \ll 1. \quad (2.108)$$

Thus, we will need both small and large argument expansions of the Maxwell integral $\psi(x)$ and its derivative $\psi'(x)$, as well as evaluation of them at the particular value of unity.

The behavior of $\psi(x)$ and other functions of interest are sketched in Fig. 2.8. For $x = 1$, we have $\psi = 0.4276$, $\psi' = 0.4151$ and $\psi + \psi' - \psi/2x = 0.6289$. Small and large argument expansions of interest in evaluating ν_S , ν_\perp , ν_\parallel , and ν_ε are:

$x \ll 1$

$$\begin{aligned} \psi(x) &\simeq (4x^{3/2}/3\sqrt{\pi})(1 - 3x/5 + 3x^2/14 - \dots), \\ \psi' &= (2\sqrt{x}e^{-x}/\sqrt{\pi}) \simeq (2x^{1/2}/\sqrt{\pi})(1 - x + x^2/2 - \dots), \\ \psi + \psi' - \psi/2x &\simeq (4x^{1/2}/3\sqrt{\pi})(1 - x/5 + 3x^2/70 - \dots), \end{aligned} \quad (2.109)$$

Figure 2.8: Maxwell integral $\psi(x)$ and related functions.

$x \gg 1$

$$\begin{aligned}
 \psi(x) &\simeq 1 - (2\sqrt{x} e^{-x}/\sqrt{\pi})(1 + 1/2x - 1/4x^2 + \dots), \\
 \psi'(x) &= 2\sqrt{x} e^{-x}/\sqrt{\pi}, \\
 \psi + \psi' - \psi/2x &\simeq 1 - 1/2x + (e^{-x}/\sqrt{\pi} x^{3/2})(1 - 1/x + \dots).
 \end{aligned} \tag{2.110}$$

Using only the lowest order of these approximations in (2.89)–(2.92), we find the relationships between various collisional processes listed in Table 2.1. The rates are all referred to the electron-ion collision frequency $\nu_0^{e/i}$, which is the same as the Lorentz collision frequency in (2.14). The $\nu_S^{e/i}$ and $\nu_\perp^{e/i}$ components of the first (e/i) column are the same as those given by the Lorentz collision model [cf., (2.13) and (2.19)]. All the other electron processes indicated in the table arise from the finite mass ratio between the electrons and ions, and the fact that the background particles are in motion. Note that in this general collision model the electron-ion parallel (speed) diffusion ($\nu_\parallel^{e/i}$) and energy loss ($\nu_\varepsilon^{e/i}$) are of order $m_e/m_i \ll 1$ compared to the Lorentz collision model processes — because of the inefficiency of energy transfer in collisions of particles with very disparate masses.

From Table 2.1 we see that the various collisional processes naturally split into three groups of rates: $\nu_0^{e/i}$, $Z_i^2 \sqrt{m_e/m_i} \nu_0^{e/i}$, and $Z_i(m_e/m_i) \nu_0^{e/i}$. The fastest of these rates is the Lorentz collision rate; however, all the electron-electron collisional processes also occur at roughly the same rate and so should also be taken into account in investigations of electron collisional processes. (The electron-electron collision processes are small in a plasma where the ions all have high charge states $Z_i \gg 1$ since then $\nu_0^{e/i} = Z_i \nu_0^{e/e} \gg \nu_0^{e/e}$.) Physically, on this fastest time scale of $1/\nu_0^{e/i}$, electron momentum is relaxed by collisions

Table 2.1: Relative Coulomb collision rates for thermal speed test electrons and ions with charge Z_i in a Maxwellian plasma with $T_e = T_i$.

		e/i	e/e	i/i	i/e
slowing down	$\nu_S^{s/s'}/\nu_0^{e/i}$	1	$\frac{0.86}{Z_i}$	$0.86Z_i^2\sqrt{\frac{m_e}{m_i}}$	$0.75Z_i\frac{m_e}{m_i}$
perpendicular diffusion	$\nu_\perp^{s/s'}/\nu_0^{e/i}$	2	$\frac{1.26}{Z_i}$	$1.26Z_i^2\sqrt{\frac{m_e}{m_i}}$	$1.50Z_i\frac{m_e}{m_i}$
speed diffusion	$\nu_\parallel^{s/s'}/\nu_0^{e/i}$	$\frac{m_e}{m_i}$	$\frac{0.43}{Z_i}$	$0.43Z_i^2\sqrt{\frac{m_e}{m_i}}$	$0.75Z_i\frac{m_e}{m_i}$
energy loss	$\nu_\varepsilon^{s/s'}/\nu_0^{e/i}$	$2\frac{m_e}{m_i}$	$\frac{0.03}{Z_i}$	$0.03Z_i^2\sqrt{\frac{m_e}{m_i}}$	$-0.75Z_i\frac{m_e}{m_i}$

on both electrons and ions, and the electrons relax within themselves through all the processes. The electron-electron collisions relax the electrons toward a Maxwellian distribution (see Chapter 11). On the next lower rate or longer time scale — by a factor of order $\sqrt{m_i/m_e} \gtrsim 43 \gg 1$ — ion-ion collisions relax the ions toward a Maxwellian distribution. Finally, on the longest time scale, which is a factor of about $m_i/m_e \gtrsim 1836 \gg 1$ slower than $1/\nu_0^{e/i}$, there is energy transfer between the electrons and ions, and ion momentum loss to the electrons. [The energy loss rate $\nu_\varepsilon^{i/e}$ is negative here because we are evaluating it for a test particle whose energy $mv^2/2 = T$ is less than the average particle energy in the plasma, $m\bar{v}^2/2 = 3T/2$ — see (??) in Appendix A.4].

2.10 Plasma Collision Rates+

Next, we consider the overall collisional relaxation rates for the entire electron and ion species of charged particles in a plasma. First, we consider the temperature equilibration rate for a Maxwellian distribution of test particles of species s colliding with a Maxwellian distribution of background particles s' . Multiplying the test particle energy loss equation defined in the last line of (2.87) by an isotropic Maxwellian velocity distribution of test particles s in the form given in (2.75) and using the first property of ψ given in (2.79) to integrate the ψ contribution to the $\nu_\varepsilon^{s/s'}$ defined in (2.92) by parts once, we find

$$\frac{3}{2}n_s\frac{dT_s}{dt} = -\bar{\nu}_\varepsilon^{s/s'}n_s(T_s - T_{s'}), \quad (2.111)$$

where

$$n_s \bar{\nu}_{\mathcal{E}}^{s/s'} = n_s \frac{m_s}{m_{s'}} \left[\frac{4}{\sqrt{\pi}} \nu_0^{s/s'}(v_{T_{ss'}}) \right] = n_{s'} \bar{\nu}_{\mathcal{E}}^{s'/s} = \frac{4}{\sqrt{\pi}} \frac{4\pi n_s n_{s'} q_s^2 q_{s'}^2 \ln \Lambda_{ss'}}{\{4\pi\epsilon_0\}^2 m_s m_{s'} v_{T_{ss'}}^3}, \quad (2.112)$$

is the average energy density exchange rate between the species. Here,

$$v_{T_{ss'}} \equiv [2(T_s/m_s + T_{s'}/m_{s'})]^{1/2} = \sqrt{v_{T_s}^2 + v_{T_{s'}}^2} \quad (2.113)$$

is the appropriate mean thermal velocity for a combination of test and background particles, both with Maxwellian distributions. From the equality of $n_s \bar{\nu}_{\mathcal{E}}^{s/s'}$ and $n_{s'} \bar{\nu}_{\mathcal{E}}^{s'/s}$, it is obvious that

$$n_s \frac{dT_s}{dt} = -n_{s'} \frac{dT_{s'}}{dt}, \quad (2.114)$$

as required by energy conservation — energy lost from the test particle species is gained by the (dissimilar) background species with which it suffers Coulomb collisions. For a couple of applications of these temperature equilibration formulas see Problems 2.35 and 2.36.

For typical electron-ion plasmas where $m_e \ll m_i$ and T_e is not too different from T_i so that $T_e/m_e \gg T_i/m_i$ ($v_{T_e} \gg v_{T_i}$), (2.111) becomes [cf., (2.38)]

$$\frac{3}{2} n_e \frac{dT_e}{dt} = -\bar{\nu}_{\mathcal{E}}^{e/i} n_e (T_e - T_i) = -3 \frac{m_e}{m_i} n_e \nu_e (T_e - T_i) \equiv -Q_i. \quad (2.115)$$

In the next to last expression we have used the fundamental ν_e defined in (2.17). The relevant formula for the electron-ion energy transfer rate $\bar{\nu}_{\mathcal{E}}^{e/i}$ in a plasma with impurities (see Problem 2.39) was given previously in (2.48) and (2.49).

Finally, we calculate the momentum relaxation rate for two Maxwellian distributions of particles that are drifting (flowing) slowly relative to each other with velocity $\mathbf{V} \equiv \mathbf{V}_s - \mathbf{V}_{s'}$, assuming $|\mathbf{V}| \ll v_{T_{ss'}}$. In the rest frame of the background particles (s'), the drifting test particle (s) distribution function can be written as in (2.15):

$$\begin{aligned} f_s(\mathbf{v}) &= n_s \left(\frac{m_s}{2\pi T_s} \right)^{3/2} \exp \left(-\frac{m_s |\mathbf{v} - \mathbf{V}|^2}{2T_s} \right) \\ &\simeq \frac{n_s e^{-v^2/v_{T_s}^2}}{\pi^{3/2} v_{T_s}^3} \left[1 + \frac{2\mathbf{v} \cdot \mathbf{V}}{v_{T_s}^2} + \dots \right]. \end{aligned} \quad (2.116)$$

Multiplying the momentum loss rate formula in the first line of (2.87) by this distribution function and integrating over velocity space, again integrating once by parts and using the first relation in (2.79), we find

$$m_s n_s \frac{d\mathbf{V}_s}{dt} = -\bar{\nu}_S^{s/s'} m_s n_s (\mathbf{V}_s - \mathbf{V}_{s'}), \quad (2.117)$$

where

$$m_s n_s \bar{\nu}_S^{s/s'} = m_s n_s \left[\frac{4}{3\sqrt{\pi}} \frac{m_s}{m_{ss'}} \nu_0^{s/s'}(v_{T_{ss'}}) \right] = \frac{4}{3\sqrt{\pi}} \frac{4\pi n_s n_{s'} q_s^2 q_{s'}^2 \ln \Lambda_{ss'}}{\{4\pi\epsilon_0\}^2 m_{ss'} v_{T_{ss'}}^3} \quad (2.118)$$

is the average momentum density exchange rate between the s and s' species of particles, and $v_{T_{ss'}}$ is the average thermal velocity defined in (2.113). From the symmetric form of $m_s n_s \bar{\nu}_S^{s/s'}$ in terms of the species labels s and s' , it is clear that the momentum lost from the s species is gained by the s' species and thus momentum is conserved in the Coulomb collisional interactions between the two species of particles: $m_s n_s d\mathbf{V}_s/dt = -m_{s'} n_{s'} d\mathbf{V}_{s'}/dt$.

Specializing again to an electron-ion plasma and assuming as usual that $v_{T_e} \gg v_{T_i}$, we find that (2.117) and (2.118) reduce to [cf., (2.34)]

$$m_e n_e \frac{d\mathbf{V}_e}{dt} = -m_e n_e \nu_e (\mathbf{V}_e - \mathbf{V}_i) \equiv \mathbf{R}_e, \quad (2.119)$$

where

$$\nu_e = \bar{\nu}_S^{e/i} = \frac{4}{3\sqrt{\pi}} \nu_0^{e/i}(v_{T_e}) = \frac{4\sqrt{2\pi} n_e Z_i e^4 \ln \Lambda}{\{4\pi\epsilon_0\}^2 3 m_e^{1/2} T_e^{3/2}} \equiv \frac{1}{\tau_e}. \quad (2.120)$$

This electron momentum relaxation rate is the same as that obtained in (2.17) for the Lorentz collision model and shows that the fundamental Maxwellian-averaged electron-ion collision frequency ν_e is in fact $\bar{\nu}_S^{e/i}$. Electron-electron collisions do not contribute to the momentum relaxation process because they are momentum conserving for the electron species as a whole. Note also that the collisional momentum relaxation process acts on the difference between the electron and ion flow velocities. Thus, the net effect of Coulomb collisions is to relax the electron flow to the ion flow velocity. Finally, the relevant formula for the electron-ion collisional “slowing down” rate $\bar{\nu}_S^{e/i}$ in a plasma with impurities is just $\nu_e = Z_{\text{eff}} \bar{\nu}_S^{e/Z_i=1}$ [see (2.44) and Problem 2.37].

For the slightly fictitious case of two ion species with charge $q_i = Z_i e$ that have equal temperatures but are drifting relative to each other with velocity \mathbf{V} , the ion momentum relaxation rate is given by

$$m_i n_i \frac{d\mathbf{V}}{dt} = -m_i n_i \nu_i \mathbf{V}, \quad (2.121)$$

where [cf., (2.36)]

$$\nu_i = \bar{\nu}_S^{i/i} = \frac{4\sqrt{\pi} n_i Z_i^4 e^4 \ln \Lambda}{\{4\pi\epsilon_0\}^2 3 m_i^{1/2} T_i^{3/2}} \equiv \frac{1}{\tau_i}. \quad (2.122)$$

As can be anticipated from the $\nu_S^{i/i}$ entry in Table 2.1, this momentum relaxation rate is a factor of order $Z_i^2 \sqrt{m_e/m_i}$ slower than that for electrons. Also, the ion-electron collisional effects due to $\nu_S^{i/e}$ have been neglected in the average ion momentum loss rate because they are a factor of order $\sqrt{m_e/m_i}$ smaller than the ion-ion collisional effects. The numerical factor in (2.122) is $\sqrt{2}$ smaller than

that in (2.120) because of the rest mass and average thermal velocity factors for this equal mass case. Finally, the relevant formula for the ion-ion collisional “slowing down” rate $\bar{\nu}_S^{i/i}$ in a plasma with impurities (see Problem 2.38) was given in (2.45).

2.11 Fast Ion Thermalization+

In attempting to heat plasmas one often introduces “fast” ions (through absorption of energetic neutrals, from radiofrequency wave heating, or directly as energetic charged fusion products such as α particles), which have speeds intermediate between the ion and electron thermal speeds. These fast ions heat the plasma by transferring their energy to the background plasma electrons and ions during the Coulomb collision slowing down process. This collisional fast ion slowing down and energy transfer process will now be considered in detail.

For simplicity we consider an electron-hydrogenic (proton, deuteron or triton — $m_i = 1, 2$ or 3 but $Z_i = 1$) background plasma in which both species have a Maxwellian velocity distribution. The electron and ion temperatures will be assumed to be unequal, but comparable in magnitude. The fast or test ion will be allowed to have a mass (m_f) and charge ($q_f = Z_f e$) different from the background ions. Because the fast ion speed is intermediate between the electron and ion thermal speeds, the relative speed parameters in (2.81) for the fast ion-ion (f/i) and fast ion-electron (f/e) collisions are given by

$$x^{f/i} = \frac{m_i v^2}{2T_i} = \frac{v^2}{v_{Ti}^2} \gg 1, \quad x^{f/e} = \frac{m_e v^2}{2T_e} = \frac{v^2}{v_{Te}^2} \ll 1, \quad (2.123)$$

in which v is the fast ion speed. From (2.86) we see that the reference collision frequencies $\nu_0^{f/s'}$ are equal for the electron-hydrogenic ion background plasma:

$$\nu_0^{f/i} = \nu_0^{f/e}. \quad (2.124)$$

Using the approximations (2.123) in (2.109) and (2.110), we find that the fast ion transfers energy to the plasma electrons and ions at the rates defined in (2.92), which are given to lowest significant order by

$$\nu_\varepsilon^{f/i} \simeq 2 \frac{m_f}{m_i} \nu_0^{f/i}, \quad (2.125)$$

$$\nu_\varepsilon^{f/e} \simeq 2 \frac{m_f}{m_e} \frac{4(x^{f/e})^{3/2}}{3\sqrt{\pi}} \nu_0^{f/e} = 2 \frac{m_f}{m_e} \frac{4}{3\sqrt{\pi}} \frac{v^3}{v_{Te}^3} \nu_0^{f/e}. \quad (2.126)$$

From the definition of $\nu_0^{f/s'}$ in (2.86) we see that it depends on v^{-3} . Thus, $\nu_\varepsilon^{f/i}$ also depends on v^{-3} . However, $\nu_\varepsilon^{f/e}$ is independent of the fast ion speed v — because the appropriate relative speed for fast ion-electron collisions when the fast ion speed v is slower than v_{Te} is the electron thermal speed.

Adding together the fast ion energy losses via collisions with background plasma ions and electrons, the total fast ion energy loss rate becomes

$$\frac{d\varepsilon}{dt} = - \left(\nu_{\varepsilon}^{f/e} + \nu_{\varepsilon}^{f/i} \right) \varepsilon, \quad (2.127)$$

in which

$$\varepsilon = m_f v^2 / 2 \quad (2.128)$$

is the instantaneous fast ion energy. Since $\nu_{\varepsilon}^{f/e}$ is independent of the fast ion energy, it is convenient to define a characteristic fast ion slowing down time in terms of it:

$$\tau_S \equiv \frac{2}{\nu_{\varepsilon}^{f/e}} \simeq \frac{1}{\nu_S^{f/e}} = \frac{m_f}{m_e} \frac{\{4\pi\epsilon_0\}^2 3 m_e^{1/2} T_e^{3/2}}{(4\sqrt{2}\pi) n_e Z_f^2 e^4 \ln \Lambda} = \left(\frac{m_f}{m_e} \right) \frac{1}{\nu_e}, \quad (2.129)$$

$$\text{fast ion slowing down time.} \quad (2.130)$$

Here, the approximate equality to $1/\nu_S^{f/e}$ follows because for $m_f/m_e \gg 1$ the fast ions are not significantly scattered by the electrons; thus, they lose energy to the plasma electrons at twice the rate they lose momentum to them.

The rate of transfer of fast ion energy to plasma ions can be referenced to the transfer rate to the electrons in terms of a critical energy $\varepsilon_c \equiv m_f v_c^2 / 2$ as follows:

$$\frac{\nu_{\varepsilon}^{f/i}}{\nu_{\varepsilon}^{f/e}} = \left(\frac{\varepsilon_c}{\varepsilon} \right)^{3/2} = \frac{v_c^3}{v^3}, \quad (2.131)$$

where

$$\varepsilon_c \equiv \frac{m_f v_c^2}{2} = T_e \left[\frac{3\sqrt{\pi}}{4} \sqrt{\frac{m_f}{m_e}} \frac{m_f}{m_i} \right]^{2/3} \simeq 15 T_e \left(\frac{m_f}{m_p^{1/3} m_i^{2/3}} \right) \quad (2.132)$$

in which m_p is the proton mass. (For the appropriate modifications when multiple species of ions are present, see Problems 2.40 and 2.50.) In terms of this critical energy, (2.127) can be written as

$$\frac{d\varepsilon}{dt} = - \frac{2\varepsilon}{\tau_S} \left[1 + \left(\frac{\varepsilon_c}{\varepsilon} \right)^{3/2} \right]. \quad (2.133)$$

The fast ion energy transfer rates as a function of energy are illustrated in Fig. 2.9. For fast ion energies greater than ε_c the energy transfer is primarily to electrons, while for $\varepsilon < \varepsilon_c$ it is primarily to ions.

Since (2.133) applies for all fast ion speeds between the electron and ion thermal speeds, it will be valid for all fast ion energies during the thermalization process. Thus, its solution will give the fast ion energy as a function of time as it transfers its energy to the background plasma. To solve (2.133) it is convenient to convert it to an equation for the fast ion speed $v \equiv \sqrt{2\varepsilon/m_f}$, for which it becomes

$$\frac{dv}{dt} = - \frac{v}{\tau_S} \left[1 + \frac{v_c^3}{v^3} \right], \quad (2.134)$$

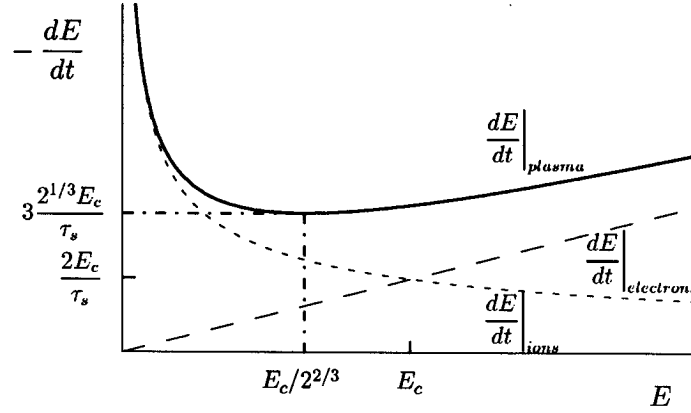


Figure 2.9: Fast ion energy transfer rate versus energy ε . The energy transfer is primarily to electrons for $\varepsilon > \varepsilon_c$, but to ions for $\varepsilon < \varepsilon_c$.

$$v_c \equiv \sqrt{\frac{2\varepsilon_c}{m_f}} = \left[\frac{3\sqrt{\pi}}{4} \frac{m_e}{m_i} \right]^{1/3} v_{Te}. \quad (2.135)$$

Multiplying (2.134) by v^2 and integrating over time from $t = 0$ where the initial fast ion speed will be taken to be v_0 to the current time t where it has speed v (assumed $> v_{Ti}$), we obtain

$$t = \frac{\tau_S}{3} \ln \left(\frac{v_0^3 + v_c^3}{v^3 + v_c^3} \right), \quad (2.136)$$

or

$$v^3(t) = (v_0^3 + v_c^3) e^{-3t/\tau_S} - v_c^3. \quad (2.137)$$

The fast ion energy $\varepsilon(t) = m_f v^2(t)/2$ during the slowing down process can be readily obtained from this last result.

The decay of the fast ion energy with time is illustrated in Fig. 2.10. Note that for initial energies much greater than the critical energy ε_c the fast ion energy decays exponentially in time at a rate $2/\tau_S = \nu_{\varepsilon}^{f/e}$ due to collisions with electrons, as is apparent from (2.133). However, when the fast ion energy drops below ε_c the energy transfer is predominantly to the ions and the fast ion energy decays much faster than exponentially. The total lifetime for thermalization (i.e., to $v \simeq v_{Ti} \ll v_c$) of the fast ion into the background plasma ions is

$$\tau_f \simeq (\tau_S/3) \ln [1 + (\varepsilon_0/\varepsilon_c)^{3/2}] = (\tau_S/3) \ln [1 + v_0^3/v_c^3]. \quad (2.138)$$

A couple of applications of these fast ion slowing down effects and formulas are developed in Problems 2.41 and 2.42.

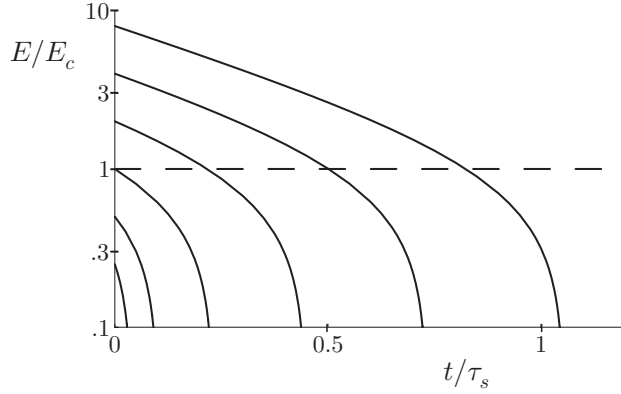


Figure 2.10: Decay of fast ion energy ε versus time during thermalization into a background plasma for various initial ratios of ε to the critical energy ε_c .

Next, we calculate the fraction of the fast ion energy transferred to the background plasma electrons and ions over the entire fast ion slowing down process. Since in many plasma situations the fast ions are also susceptible to other, direct loss processes such as charge-exchange, we introduce a probability $\exp(-t/\tau_{\text{cx}})$ that the fast ion will remain in the plasma for a time t against charge-exchange losses at rate $1/\tau_{\text{cx}}$. Then, the fraction G_e of the total fast ion energy $\varepsilon_0 \equiv m_f v_0^2/2$ transferred to the electrons during the thermalization process is given by

$$G_e \equiv \frac{1}{\varepsilon_0} \int_0^{\tau_f} dt \left(-\frac{d\varepsilon}{dt} \right) \frac{\nu_{\varepsilon}^{f/e} e^{-t/\tau_{\text{cx}}}}{\nu_{\varepsilon}^{f/e} + \nu_{\varepsilon}^{f/i}} = \frac{2}{v_0^2} \int_0^{v_0} \frac{v^3}{v^3 + v_c^3} v dv \left[\frac{v^3 + v_c^3}{v_0^3 + v_c^3} \right]^{\tau_S/3\tau_{\text{cx}}} \quad (2.139)$$

Similarly, the fraction G_i of fast ion energy transferred to the ions is (for the simpler case where $\tau_{\text{cx}} \rightarrow \infty$, see also the form given in Problem 2.43)

$$G_i \equiv \frac{1}{\varepsilon_0} \int_0^{\tau_f} dt \left(-\frac{d\varepsilon}{dt} \right) \frac{\nu_{\varepsilon}^{f/i} e^{-t/\tau_{\text{cx}}}}{\nu_{\varepsilon}^{f/e} + \nu_{\varepsilon}^{f/i}} = \frac{2}{v_0^2} \int_0^{v_0} \frac{v^3}{v^3 + v_c^3} v dv \left[\frac{v^3 + v_c^3}{v_0^3 + v_c^3} \right]^{\tau_S/3\tau_{\text{cx}}} \quad (2.140)$$

The fraction of fast ion energy lost due to charge-exchange is $1 - G_i - G_e$. However, a portion of this energy may be absorbed in the plasma if some of the fast neutrals produced by charge-exchange are reabsorbed before they leave the plasma.

The fractions G_e, G_i of fast ion energy transferred to plasma electrons and ions during the thermalization process as a function of $\varepsilon_0/\varepsilon_c$ is illustrated in Fig. 2.11. Note that the integrated fractions G_i, G_e become equal for $\varepsilon_0 \lesssim 2\varepsilon_c$, which is significantly larger than the value of $\varepsilon_0 \simeq \varepsilon_c$ where the instantaneous energy transfer rates are equal — recall Fig. 2.9. Also, charge-exchange losses become significant for $\tau_S/\tau_{\text{cx}} \gtrsim 1$, and can greatly diminish the fast ion energy

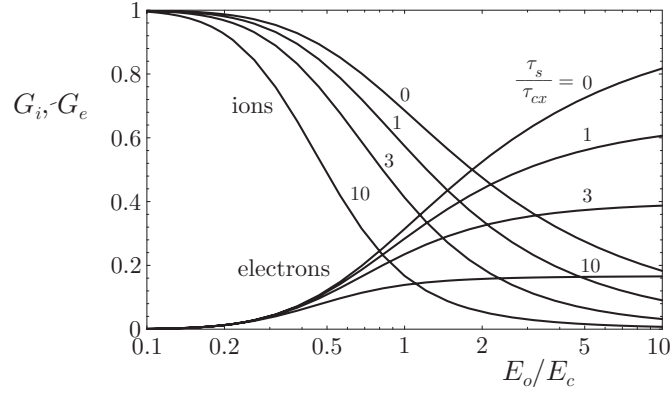


Figure 2.11: Fraction of the fast ion energy ε_0 transferred to background plasma electrons (G_e) and ions (G_i) as a function of the ratio of the initial energy ε_0 to the critical energy ε_c . The variation with τ_s/τ_{cx} indicates the influence of direct fast ion losses (at rate $1/\tau_{cx}$) during the thermalization process.

transfer to the plasma for $\tau_s/\tau_{cx} \gg 1$. For some typical applications of fast ion slowing down and energy transfer processes and their effects on plasmas, see Problems 2.44–2.47. One key result for fusion experiments is that for 3.52 keV alpha particles slowing down in a $T_e \sim 10$ keV deuterium-tritium plasma for which $\varepsilon_c \sim 330$ keV we obtain $\varepsilon_0/\varepsilon_c \sim 10$ and hence (from Fig. 2.11) the alpha particle deposits over 80% of its energy in the plasma electrons.

In addition to energy loss, the fast ions experience perpendicular and parallel diffusion in velocity space during their thermalization. The relative importance of the various Coulomb collision processes on the fast ion for the conditions given in (2.123) are indicated in Table 2.2. From this table we see that for $\varepsilon \gg \varepsilon_c$ the momentum and energy losses by the fast ions to the electrons are the dominant processes because then the velocity space diffusion effects indicated by ν_\perp, ν_\parallel are small. However, for $\varepsilon < \varepsilon_c$ the fast ions lose energy primarily to the background ions and their perpendicular or angular diffusion rate in velocity space becomes equal to their energy loss rate. For some typical applications of fast ion scattering processes and their effects on plasmas, see Problems 2.48–2.50.

The energy or speed diffusion process indicated by ν_\parallel is negligible until the fast ion energy is reduced to approximately the ion temperature in the background plasma. Since the energy diffusion process is thus negligible during the fast ion thermalization process, and the perpendicular diffusion has no effect on the energy transfer rates, our characterization of the fast ion slowing down process as one of a monotonic decrease in the fast ion energy is a reasonably accurate one. A kinetic description that allows for pitch-angle (ϑ) scattering along with the fast ion energy loss process is developed in Section 11.4.

Table 2.2: Relative Coulomb collision rates for fast ions with $v_{Ti} \ll v \ll v_{Te}$ slowing down in a plasma with Maxwellian electrons and ions ($\varepsilon_c \sim 15 T_e$).

		$\frac{f/i}{\quad}$	$\frac{f/e}{\quad}$
slowing down	$\nu_S^{f/s'}/\nu_0^{f/e}$	$\left(1 + \frac{m_f}{m_i}\right)$	$\frac{m_f}{m_e} \frac{4}{3\sqrt{\pi}} \left(\frac{v}{v_{Te}}\right)^3 = \left(\frac{\varepsilon}{\varepsilon_c}\right)^{3/2}$
perpendicular diffusion	$\nu_{\perp}^{f/s'}/\nu_0^{f/e}$	2	$\frac{8}{3\sqrt{\pi}} \left(\frac{v}{v_{Te}}\right) \ll 1$
speed diffusion	$\nu_{\parallel}^{f/s'}/\nu_0^{f/e}$	$\frac{T_i}{m_f v^2/2} \ll 1$	$\frac{4}{3\sqrt{\pi}} \left(\frac{v}{v_{Te}}\right) \ll 1$
energy loss	$\nu_{\varepsilon}^{f/s'}/\nu_0^{f/e}$	$2 \frac{m_f}{m_i}$	$\frac{m_f}{m_e} \frac{8}{3\sqrt{\pi}} \left(\frac{v}{v_{Te}}\right)^3 = 2 \left(\frac{\varepsilon}{\varepsilon_c}\right)^{3/2}$

REFERENCES AND SUGGESTED READING

The basic Coulomb collision processes were first worked out in the analogous context (see Problem 2.9) of the gravitational interaction of stars:

Chandrasekhar, *Principles of Stellar Dynamics* (1942).

S. Chandrasekhar, *Rev. Mod. Phys.* **15**, 1 (1943).

A comprehensive application to Coulomb collisions in a plasma was first presented in Spitzer, *Physics of Fully Ionized Gases* (1962).

The most general development of the dynamical friction and velocity diffusion coefficients for a plasma in terms of the Rosenbluth potentials originated in the paper

M.N. Rosenbluth, W. MacDonald and D. Judd, *Phys. Rev.* **107**, 1 (1957).

The most comprehensive treatments of the Coulomb collision effects on test particles in a plasma are found in

B.A. Trubnikov, “Particle Interactions in a Fully Ionized Plasma,” in *Reviews of Plasma Physics*, M.A. Leontovich, ed. (Consultants Bureau, New York, 1965), Vol. I, p. 105.

D.V. Sivukhin, “Coulomb Collisions in a Fully Ionized Plasma,” in *Reviews of Plasma Physics*, M.A. Leontovich, ed. (Consultants Bureau, New York, 1966), Vol. IV, p. 93.

A brief, but very useful summary of the important Coulomb collision formulas in this chapter is given in

Book, *NRL Plasma Formulary* (1990), p. 31.

A book devoted almost entirely to the subject of Coulomb collision effects in a plasma in which numerous examples are worked out is

Shkarofsky, Johnston and Bachynski, *The Particle Kinetics of Plasmas* (1966).

Also, most books on plasma physics have chapters devoted to discussions of Coulomb collision effects. Among the most descriptive and useful are those in

- Spitzer, *Physics of Fully Ionized Gases* (1962), Chapter 5
- Rose and Clark, *Plasmas and Controlled Fusion* (1961), Chapter 8.
- Schmidt, *Physics of High Temperature Plasmas* (1979), Chapter 11.
- Krall and Trivelpiece, *Principles of Plasma Physics* (1973), Chapter 6.
- Golant, Zhilinsky and Sakharov, *Fundamentals of Plasma Physics* (1980), Chapter 2.

The original theory of runaway electrons was developed in

- H. Dreicer, *Proceedings of the Second United Nations International Conference on the Peaceful Use of Atomic Energy* (United Nations, Geneva, 1958), Vol. 31, p. 57. See also, *Phys. Rev.* **115**, 238 (1959).

The thermalization of a fast ion in a Maxwellian plasma was first developed in

- D.J. Sigmar and G. Joyce, *Nuclear Fusion* **11**, 447 (1971).
- T.H. Stix, *Plasma Physics* **14**, 367 (1972).

Inclusion of charge-exchange loss and geometry effects on neutral-beam-injected fast ions are discussed in

- J.D. Callen, R.J. Colchin, R.H. Fowler, D.G. McAlees and J.A. Rome, “Neutral Beam Injection into Tokamaks,” *Plasma Physics and Controlled Nuclear Fusion Research 1974* (IAEA, Vienna, 1975), Vol. I, p. 645.

The Monte Carlo computational approach to including Coulomb collisional effects has been developed primarily in the context of investigating transport processes in

- R. Shanny, J.M. Dawson and J.M. Greene, *Phys. Fluids* **10**, 1281 (1967).
- K.T. Tsang, Y. Matsuda and H. Okuda, *Phys. Fluids* **18**, 1282 (1975).
- T. Takizuka and H. Abe, *J. Comput. Phys.* **25**, 205 (1977).
- A.H. Boozer and G. Kuo-Petravic, *Phys. Fluids* **24**, 851 (1981).

PROBLEMS

- 2.1 Consider the length scales relevant for electron Coulomb collision processes in a typical university-scale magnetic fusion plasma experiment that has $n_e = 2 \times 10^{13} \text{ cm}^{-3}$ and $T_e = T_i = 1 \text{ keV}$. Calculate: a) the distance of closest approach b_{\min} ; b) the average interparticle spacing; c) the maximum interaction distance b_{\max} ; and d) the average collision length $\lambda_e = v_{Te}/\nu_e$ for electrons in this plasma. What is the ratio of each of these lengths to the mean interparticle spacing? /
- 2.2 Consider the length scales relevant for electron Coulomb collision processes in a laser-produced electron-proton plasma that has $n_e = 10^{29} \text{ m}^{-3}$ and $T_e = T_i = 1 \text{ keV}$. Calculate: a) the distance of closest approach b_{\min} ; b) the average interparticle spacing; c) the maximum interaction distance b_{\max} ; and d) the average collision length $\lambda_e = v_{Te}/\nu_e$ for electrons in this plasma. What is the ratio of each of these lengths to the mean interparticle spacing? /
- 2.3 Estimate the time scales relevant for electron Coulomb collision processes in the earth’s ionosphere at a point where $n_e = 10^{12} \text{ m}^{-3}$, $T_e = 1 \text{ eV}$. For simplicity, use a Lorentz collision model and assume the ions have $Z_i = 1$ and $T_i \simeq T_e$. Calculate the times for: a) a typical Coulomb interaction at the average interparticle spacing; b) an electron to traverse the Debye shielding cloud; and c) the average electron collision time $\tau_e = 1/\nu_e$. How long (or short) are each of these times compared to the “plasma period” ω_{pe}^{-1} ? /

- 2.4 Consider the “slowing down” of an electron using the Lorentz collision model. a) Show that an electron with an initial velocity \mathbf{v}_0 loses momentum exponentially in time at a decay rate given by $\nu(v_0)$. b) What is the electron energy after its momentum is totally depleted? c) Calculate the distance the electron travels in its original direction of motion while losing its momentum. d) Evaluate the momentum decay rate and distance the electron travels for a plasma with $Z_i = 5$, $n_e = 10^{19} \text{ m}^{-3}$, $T_e = T_i = 100 \text{ eV}$, and an initial electron “test particle” energy of 1 keV. [Hint: Be careful to distinguish between an electron’s velocity (a directional, vector quantity) and its speed (a scalar quantity).] //
- 2.5 In Section 2.1 we derived the momentum impulse $\Delta \mathbf{v}$ for a single Coulomb collision in the Lorentz collision model by integrating $m_e(d\mathbf{v}/dt) = q_e \mathbf{E}$ over an unperturbed “straight-line” trajectory to determine $\Delta \mathbf{v}_\perp$ and then used $\Delta v_\parallel \simeq -\Delta \mathbf{v}_\perp \cdot \Delta \mathbf{v}_\perp / 2v$. Show that the result for Δv_\parallel given in (2.6) can be obtained directly by integrating $\mathbf{E}[\mathbf{x}(t)]$ along a perturbed electron trajectory $\mathbf{x}(t) = \mathbf{x} + \tilde{\mathbf{x}}$ that includes the first order effects $\tilde{\mathbf{x}}$ due to the \mathbf{E} field of the ion on the electron trajectory. [Hint: First calculate the perturbed velocity $\tilde{\mathbf{v}}$, and then make use of the fact that

$$\begin{aligned} \Delta v_\parallel &= \hat{\mathbf{e}}_z \cdot \frac{q_e}{m_e} \int_{-\infty}^{\infty} dt \mathbf{E}(\mathbf{x} + \tilde{\mathbf{x}}) = \frac{q_e}{m_e} \int_{-\infty}^{\infty} dt \hat{\mathbf{e}}_z \cdot \left[\mathbf{E}(\mathbf{x}) + \tilde{\mathbf{x}} \cdot \frac{\partial \mathbf{E}}{\partial \mathbf{x}} \Big|_{\mathbf{x}} + \dots \right] \\ &= \frac{e}{m_e} \int_{-\infty}^{\infty} dt \tilde{\mathbf{v}} \cdot \nabla \int_{-\infty}^t E_z(t') = \frac{Z_i e^2}{\{4\pi\epsilon_0\} m_e v} \int_{-\infty}^{\infty} dt \tilde{v}_\parallel \frac{t}{(b^2 + v^2 t^2)^{3/2}}. \end{aligned} //$$

- 2.6 Show that the Lorentz collision frequency ν can be derived from the Rutherford differential scattering cross-section $d\sigma/d\Omega$ given in (??) in Appendix A.1 and Problem 2.24 as follows. a) First, show that for the Lorentz collision model the scattering angle ϑ is given for typical small-angle Coulomb collisions by $\vartheta \simeq 2Z_i e^2 / (\{4\pi\epsilon_0\} m v^2 b) = 2b_{\min}^{\text{cl}} / b$, and that the differential scattering cross-section is $d\sigma/d\Omega = |(b db d\varphi)/(d\varphi d \cos \vartheta)| \simeq (b/\vartheta) |db/d\vartheta| = 4(b_{\min}^{\text{cl}})^2 / \vartheta^4$. b) Then, determine the effective cross-section for momentum transfer σ_m , which is defined by

$$\sigma_m \equiv \int d\Omega (d\sigma/d\Omega) (1 - \cos \vartheta).$$

In performing this integral discuss the maximum, minimum scattering angles ϑ_{\max} , ϑ_{\min} in terms of the b_{\min} , b_{\max} interaction distances. c) Finally, show that $\nu = n_i \sigma_m v$ yields the Lorentz model collision frequency given in (2.14). ///

- 2.7 Use the full Rutherford differential scattering cross-section and the procedure outlined in the preceding problem to give an alternative derivation of the Lorentz collision frequency that takes into account classical “hard,” or large angle collisions; i.e., do not initially assume $\vartheta \ll 1$. ///
- 2.8 The Lorentz collision frequency ν can also be determined from the Langevin equation

$$m_e \frac{d\mathbf{v}}{dt} = -m_e \nu \mathbf{v} + \Delta \mathbf{F}(t)$$

in which $-m_e \nu \mathbf{v}$ is the dynamical friction force, and $\Delta \mathbf{F}(t)$ is a stochastic force, which for Coulomb collisions is that given by (2.2). a) Assuming ν is constant in

time, use an integrating factor $e^{\nu t}$ in solving the Langevin equation to determine the particle velocity $\mathbf{v}(t)$ after its initialization to \mathbf{v}_0 at $t = 0$. b) Next, calculate the ensemble average of the electron kinetic energy as a function of time, and show that it yields

$$\langle v^2(t) \rangle \simeq v_0^2 e^{-2\nu t} + \frac{1 - e^{-2\nu t}}{2\nu} \int_{-\infty}^{\infty} d\tau \frac{\langle \Delta \mathbf{F}(0) \cdot \Delta \mathbf{F}(\tau) \rangle}{m_e^2}.$$

c) Show that for times long compared to the duration of individual Coulomb collisions but short compared to the momentum loss collision time ($b/v \ll t \ll 1/\nu$), the electron kinetic energy is constant through terms of order νt when

$$\nu \equiv \frac{1}{2m_e^2 v^2} \int_{-\infty}^{\infty} d\tau \langle \Delta \mathbf{F}(0) \cdot \Delta \mathbf{F}(\tau) \rangle.$$

Thus, ν is proportional to the autocorrelation function of the Coulomb collision force $\Delta \mathbf{F}$. d) Next, show that for Coulomb collisions between electrons and a stationary background of randomly distributed ions this formula yields the Lorentz collision frequency given by (2.14). e) Finally, making use of the equilibrium ($\nu t \rightarrow \infty$) statistical mechanics (thermodynamics) property that for random (Brownian) motion due to a stochastic force $\Delta \mathbf{F}$ the ensemble-average kinetic energy $m_e \langle v^2 \rangle / 2$ of a particle is $T_e/2$, note that this last result yields

$$\nu = \frac{m_e}{2T_e} \int_{-\infty}^{\infty} d\tau \frac{\langle \Delta \mathbf{F}(0) \cdot \Delta \mathbf{F}(\tau) \rangle}{m_e^2}, \quad \text{fluctuation-dissipation theorem,}$$

which is also related to Nyquist's theorem for noise in electrical circuits. [Hints: a) Here, $\langle f \rangle \equiv n_i \int d^3x f = n_i \int_{-\infty}^{\infty} dz \int b db \int_0^{2\pi} d\varphi f$; b) The electron position for an ion at $\mathbf{x} = z\hat{\mathbf{e}}_z$ at time $t = 0$ is $\mathbf{x} = b(\hat{\mathbf{e}}_x \cos \varphi + \hat{\mathbf{e}}_y \sin \varphi) - (z - vt)\hat{\mathbf{e}}_z$.] ///

- 2.9 Consider cumulative small-angle collisional interactions of a test star of mass M_t and velocity \mathbf{v} in a galaxy for which the gravitational force between it and groups of field stars with density n_f and mass M_f is given by [cf., (??) in Appendix A.6] $\mathbf{F}_G = -GM_t M_f (\mathbf{x}_t - \mathbf{x}_f) / |\mathbf{x}_t - \mathbf{x}_f|^3$ — an attractive inverse square law force like that for Coulomb collisions of oppositely charged particles. a) Develop a model for collisions of this test star with other, background stars and show that the reference gravitational collision frequency analogous to (2.14) is

$$\nu_G = \frac{4\pi G^2 n_f M_f^2}{v^3} \ln \left[\frac{D_0 \overline{u^2}}{G(M_t + M_f)} \right],$$

where b_{\max} is taken to be D_0 , the mean distance between stars ($\sim n_f^{-1/3}$) and b_{\min} has been taken to be the minimum interaction distance given by an expression analogous to that implied by (2.9). b) Estimate the time in (years) for the velocity of our sun to scatter through 90° , assuming that our sun is a typical star in our galaxy which has a mass of 2×10^{30} kg, a velocity of 20 km/s and a mean separation from other stars in our galaxy of 1 parsec ($\simeq 3 \times 10^{13}$ km). c) Will you be concerned about this scattering process in your lifetime? ///

- 2.10 Estimate the diffusion coefficient D for a Fick's law representation ($\mathbf{\Gamma} = -D\nabla n$) of the particle flux $\mathbf{\Gamma}$ due to electron-ion Coulomb collision effects in an inhomogeneous plasma as follows. For simplicity, use a Lorentz collision model and

assume the electrons have a density gradient but no temperature gradient. a) Show by balancing the pressure gradient force density $-\nabla p_e = -T_e \nabla n_e$ against the frictional drag induced by Coulomb collisions that $D = T_e / m_e \nu_e = \nu_e \lambda_e^2 / 2$. b) Estimate the magnitude of this diffusion coefficient for the plasma described in Problem 2.3. c) Compare the result to the viscous diffusion coefficient for molecules of air at the earth's surface. d) Why is the diffusivity of charged particles in a plasma so much larger? //

- 2.11 a) Estimate the D-D fusion reaction rate (use $\overline{\sigma_f v} \simeq 10^{-17} \text{ cm}^3/\text{s}$) for a plasma with $T_e = T_i = 40 \text{ keV}$, and $n_e = 10^{20} \text{ m}^{-3}$. b) Compare this rate to typical electron and ion Coulomb collision rates in this fusion plasma. c) How many times do electrons and ions scatter through 90° during a typical D-D fusion in this plasma? d) How far do typical electrons and ions travel in a characteristic fusion reaction time? /
- 2.12 Consider the angular scattering of a beam of 100 eV electrons introduced into an Argon laboratory plasma that has $T_e = 3 \text{ eV}$, $T_i = 1 \text{ eV}$, $Z_i = 3$ and an electron density $n_e = 10^{19} \text{ m}^{-3}$. Using the Lorentz collision model, estimate the distance over which the beam electrons are: a) scattered through an angle of 6° ; b) scattered via small angle collisions through an angle of about 90° ; and c) deflected 90° via hard collisions. Finally, d) estimate the angle $\Delta\vartheta$ through which a beam electron is scattered in a typical Coulomb interaction when the impact parameter b is given by the mean interparticle spacing of ions. //
- 2.13 Determine the energy at which electrons “run away” in response to an electric field in an impure plasma as follows. Assume that a nearly Maxwellian plasma ($T_i \sim T_e$) is composed of electrons and various species of ions with charge Z_i , for which charge neutrality requires $n_e = \sum_i n_i Z_i$. Calculate the frictional drag force on electrons in the high energy tail ($m_e v^2 / 2 \gg T_e$) of the electron distribution. Show that the energy at which electrons run away is given by (2.27) with Z_i now replaced by the Z_{eff} defined in (2.43). Also, estimate the fraction of electrons that are runaways for $|\mathbf{E}|/E_D = 0.1$ and $Z_{\text{eff}} = 2$. //
- 2.14 As electrons become relativistic ($v \rightarrow c$) the dynamical friction force decreases less rapidly than the $1/v^2$ indicated in (2.25) and Fig. 2.6. In fact, it becomes nearly constant for $\gamma \equiv (1 - v^2/c^2)^{-1/2} \gg 1$. Then, if the electric field is weak enough, there are no runaway electrons. Determine the dynamical friction force on relativistic electrons in a nonrelativistic plasma composed of electrons and ions of charge Z_i as follows. a) First, show that the change in perpendicular momentum ($\mathbf{p} \equiv \gamma m_e \mathbf{v}$) in a single Coulomb collision is given by

$$\Delta \mathbf{p}_\perp = - \frac{2Z_i e^2}{\{4\pi\epsilon_0\}bv} (\hat{\mathbf{e}}_x \cos \varphi + \hat{\mathbf{e}}_y \sin \varphi).$$

b) Next, use the relativistic form of the total particle energy ($\mathcal{E} = \sqrt{m_e^2 c^4 + p^2 c^2}$) to show that for Coulomb scattering (constant energy) collisions between high energy electrons and background electrons or ions of mass m_i the change in parallel momentum is

$$\Delta p_\parallel \simeq - \frac{\Delta \mathbf{p}_\perp \cdot \Delta \mathbf{p}_\perp}{2p} \left[1 + \gamma \frac{m_e}{m_i} \right].$$

c) Show that the frictional force induced by Coulomb collisions of the high energy

electron with the background plasma is thus

$$\langle F_{\parallel} \rangle \simeq -\frac{4\pi n_e e^4 \ln \Lambda}{\{4\pi\epsilon_0\}^2 m_e v^2} \left(1 + \frac{1 + Z_i}{\gamma}\right).$$

d) Finally, show that for a weak electric field satisfying

$$|\mathbf{E}|/E_D < 2T_e/(m_e c^2),$$

no runaway electrons will be produced in the plasma. //+

- 2.15 Estimate the electric field strength at which the entire electron distribution function runs away as follows. a) First, assume the ions are at rest and the electrons are described by a flow-shifted Maxwellian as defined in (2.116). b) Then, transform to the electron rest frame where $\mathbf{V} = \mathbf{0}$. In this frame the ions all have a velocity $-\mathbf{V}$. c) Show that the frictional force on a test ion is given by $(m_i/m_e) m_i \nu_0^{i/e}(v) \psi^{i/e}(x) \mathbf{V}$ in which $x^{i/e} = V^2/v_{Te}^2$. d) Find the maximum of this frictional force as a function of V/v_{Te} (cf., Fig. 2.8). e) Then, use the fact that this frictional force must be equal and opposite to the maximum force on the electron distribution to estimate the critical electric field strength (in terms of the Dreicer field) for total electron runaway. f) Also, show that at this electric field strength an average electron is accelerated to roughly its thermal speed in an appropriate electron collision time. //+
- 2.16 At what electron temperature is the electrical resistivity of an electron-proton plasma with $\ln \Lambda \sim 17$ the same as that of copper at room temperature for which $\eta \simeq 1.7 \times 10^{-8} \Omega \cdot \text{m}$? /
- 2.17 In a typical university-scale tokamak experiment an electron-proton plasma with $\ln \Lambda \sim 17$ is heated to a temperature of about 300 eV by the joule or “ohmic” heating induced by an electric field of about 0.5 V/m. a) What current density (in A/cm²) does this electric field induce in such a plasma? b) What is the joule heating rate (in W/cm³)? /
- 2.18 Determine the plasma electrical impedance to an oscillating electric field as follows. a) First, assume a sinusoidal electric field oscillating at a (radian) frequency ω : $\mathbf{E}(t) = \hat{\mathbf{E}} e^{-i\omega t}$. b) Then, solve an appropriate electron fluid momentum density equation and show that the frequency-dependent electrical conductivity can be written as

$$\hat{\sigma}(\omega) = \frac{n_e e^2}{m_e (\nu_e - i\omega)}.$$

c) Over what frequency range is the plasma resistive (dissipative, real) and over what range is it reactive (imaginary)? d) What frequency ranges (in Hz) are these in the earth’s ionosphere for the parameters of Problem 2.3? //

- 2.19 The plasma electrical conductivity is modified in a plasma with neutral particles. Add a neutral friction force $-m_e n_e \nu_{en} \mathbf{V}_e$, where $\nu_{en} = n_n \bar{\sigma}_{en} \bar{v}$ is the Maxwellian-averaged electron-neutral collision frequency, to the right of (2.29) and show that in equilibrium the modified electrical resistivity is given by

$$\eta = \frac{m_e (\nu_e + \nu_{en})}{n_e e^2}. //$$

- 2.20 Determine the neutral density range over which the effects of neutral particles on the electrical conductivity can be neglected using the result given in the preceding problem as follows. The reaction rate $\overline{\sigma_{en}v}$ for ionization of atomic hydrogen by electrons is approximately (to within about a factor of two)

$$\overline{\sigma_{en}v} \simeq 1.5 \times 10^{-8} \text{ cm}^3/\text{s} \quad \text{for } 10 \text{ eV} \leq T_e \leq 10^4 \text{ eV}.$$

- a) How small must the ratio of the neutral to electron density (n_n/n_e) be to neglect electron-neutral collision effects in an electron-proton plasma for $T_e = 10, 10^2, 10^3$, and 10^4 eV? b) Explain why this density ratio varies so dramatically with electron temperature. /
- 2.21 In high neutral pressure, low temperature, partially ionized plasmas (e.g., in the “glow discharge” in fluorescent light bulbs), electron-neutral collisions compete with Coulomb collisions. In particular, they can become dominant in the high energy tail of the electron distribution function, thereby causing it to effectively vanish for energies above a “cut-off” energy. Estimate the cut-off energy for a $T_e = 3$ eV, $n_e = 10^{10} \text{ cm}^{-3}$ electron-proton plasma that has a hydrogen neutral density determined by a 3 mm Hg filling pressure, assuming an electron-ionization rate coefficient $\overline{\sigma_{en}v} = 10^{-10} \text{ cm}^3/\text{s}$ for this $T_e = 3$ eV plasma. /
- 2.22 a) Sketch the variation of the energy transfer rate Q_i in (2.38) from electrons to ions in a Maxwellian electron-proton plasma as a function of T_e/T_i . b) Find the value of T_e/T_i at which the maximum energy transfer occurs. c) Explain physically why the energy transfer rate decreases for increasing $T_e/T_i \gg 1$. /
- 2.23 Consider the thermal equilibration of an electron-ion plasma with $T_e > T_i$. a) Eliminating T_i in favor of the final temperature $T_\infty = (T_e + T_i)/2$, show that in the absence of joule heating, Eq. (2.41), which governs the electron temperature evolution, can be reduced to

$$\frac{dz}{dt} = -\frac{z-1}{\tau_\infty z^{3/2}}, \quad \tau_\infty = \frac{m_i}{m_e} \frac{\tau_e}{4} \frac{1}{z^{3/2}} = \frac{m_i}{m_e} \frac{\{4\pi\epsilon_0\}^2 3 m_e^{1/2} T_\infty^{3/2}}{16\sqrt{2}\pi n_e Z_i e^4 \ln \Lambda}$$

in which $z \equiv T_e/T_\infty$. b) Integrate this equation to obtain in general

$$-\frac{t}{\tau_\infty} = \ln \left| \frac{z^{1/2} - 1}{z^{1/2} + 1} \right| + \frac{2}{3} z^{3/2} + 2 z^{1/2} + C,$$

where C is a constant to be determined from the initial conditions. c) Estimate the temporal range over which T_e decays exponentially in time toward T_∞ and indicate the decay rate. d) Discuss the relationship of this decay rate to a simple one derivable from (2.41) with T_e fixed and $\tau_e = \text{constant}$. //

- 2.24 a) Utilize the Rutherford differential scattering cross-section

$$\frac{d\sigma}{d\Omega} = \frac{q_s^2 q_{s'}^2}{4u^4 m_{ss'}^2} \frac{1}{\sin^4 \vartheta/2}, \quad \tan \frac{\vartheta}{2} = \frac{q_s q_{s'}}{m_{ss'} u^2 b} = \frac{b_{min}^{cl}}{b},$$

in which ϑ is the scattering angle, to give an alternate derivation of the frictional drag and velocity diffusion coefficients $\langle \Delta \mathbf{v} \rangle^{s/s'}/\Delta t$ and $\langle \Delta \mathbf{v} \Delta \mathbf{v} \rangle^{s/s'}/\Delta t$ defined in (2.59), (2.60) that takes into account classical “hard,” or large angle collisions. b) Show that the results reduce to those given in (2.64) and (2.65) in the limit $\ln \Lambda \gg 1$. [Hint: $b db d\varphi = d\sigma = (d\sigma/d\Omega) d\Omega = (d\sigma/d\Omega) \sin \vartheta d\vartheta d\varphi$ and after the collision the test particle velocity in the center-of-momentum frame is given by $\mathbf{u} + \Delta \mathbf{u} = (\hat{\mathbf{e}}_x \sin \vartheta \cos \varphi + \hat{\mathbf{e}}_y \sin \vartheta \sin \varphi + \hat{\mathbf{e}}_z \cos \vartheta) u$.] ///+

- 2.25 a) Show that the rate of momentum and energy loss of a test particle of species s by collisions with background particles having an arbitrary velocity distribution $f_{s'}(\mathbf{v})$ can be written, in analogy with electrostatics, as

$$m_s \frac{d\mathbf{v}}{dt} = -Q_s \frac{\partial \Phi}{\partial \mathbf{v}}, \quad \frac{d}{dt} \left(\frac{m_s v^2}{2} \right) = Q_s \left(-\mathbf{v} \cdot \frac{\partial \Phi}{\partial \mathbf{v}} - \frac{m_{ss'}}{m_s} \Phi \right),$$

where the analogous potential Φ and charge Q_s are defined by

$$\Phi(\mathbf{v}) \equiv -H_{s'}(\mathbf{v}) = -\frac{m_s}{m_{ss'}} \int d^3v' \frac{f_{s'}(\mathbf{v}')}{|\mathbf{v} - \mathbf{v}'|}, \quad Q_s \equiv m_s \Gamma_{ss'}.$$

- b) Show that for an infinitely massive, immobile background (Lorentz collision model) these formulas reduce, in analogy with an electrostatic point charge Q_s at the origin of velocity space, to

$$m_s \frac{d\mathbf{v}}{dt} = -Q_s \frac{n_{s'}}{v^3} \mathbf{v} = -m_s \nu(v) \mathbf{v}, \quad \frac{d}{dt} \left(\frac{m_s v^2}{2} \right) = 0. \quad //+$$

- 2.26 Use the formulas derived in the preceding problem to consider collisions of a test particle s with a spherically symmetric velocity distribution of background particles that all have the same speed V : $f_{s'}(\mathbf{v}) = (n_s/4\pi V^2) \delta(v - V)$. a) Show that for these collisional processes the analogous potential Φ is given by

$$\Phi = \frac{m_s}{m_{ss'}} n_{s'} \begin{cases} 1/V, & v < V, \\ 1/v, & v > V. \end{cases}$$

- b) Calculate the momentum and energy loss rates for test particle (s) speeds $v < V$, and $v > V$. c) Discuss the results obtained in analogy with electrostatics, and in particular explain by analogy with electrostatics why the test particle s exchanges no momentum with the background when $v < V$. $///+$

- 2.27 In the original work on stellar collisions Chandrasekhar introduced the function

$$G(z) \equiv \frac{\Phi(z) - z\Phi'(z)}{2z^2}, \quad \text{where } \Phi(z) \equiv \frac{2}{\sqrt{\pi}} \int_0^z dy e^{-y^2} = \text{erf}(z).$$

Show that this “Chandrasekhar function” G is related to the Maxwell integral ψ by

$$G(\sqrt{x}) = \frac{\psi(x) v_{Ts'}^2}{2v^2} = \frac{\psi}{2x},$$

and hence that the various collision frequencies for Coulomb collisions of a test particle of species s with a Maxwellian distribution of background particles of species s' can be written as

$$\begin{aligned} \nu_S^{s/s'} &= \nu_{ss'} \left(\frac{2T_s}{T_{s'}} \right) \left(1 + \frac{m_{s'}}{m_s} \right) \frac{G(v/v_{Ts'})}{(v/v_{Ts})}, \\ \nu_{\perp}^{s/s'} &= 2\nu_{ss'} [\Phi(v/v_{Ts'}) - G(v/v_{Ts'})] (v_{Ts}^3/v^3), \\ \nu_{\parallel}^{s/s'} &= 2\nu_{ss'} G(v/v_{Ts'}) (v_{Ts}^3/v^3) \end{aligned}$$

in which

$$\nu_{ss'} \equiv \nu_0^{s/s'}(v) \frac{v^3}{v_{Ts}^3} = \frac{4\pi n_{s'} q_s^2 q_{s'}^2 \ln \Lambda_{ss'}}{m_s^2 v_{Ts}^3}$$

is a reference collision frequency which has the advantage of being independent of the particle speed v . $///+$

- 2.28 Discuss the changes that occur in Problem 2.4 when general Coulomb collisions are allowed for instead of the Lorentz collision model. In particular, indicate the approximate magnitude and direction of changes in the momentum decay rate, the distance traveled and the rate of energy transfer to the ions for the plasma parameters indicated. //+
- 2.29 Consider the Coulomb collision scattering processes on a $D-T$ fusion-produced α particle ($\varepsilon_0 = 3.52$ MeV) in a thermonuclear plasma (50% D , 50% T , $T_e = T_i = 10$ keV, $n_e = 10^{20} \text{ m}^{-3}$). a) Calculate the collision rates for slowing down (ν_S), perpendicular diffusion (ν_\perp), parallel diffusion (ν_\parallel) and energy loss (ν_ε) of the α particle in the plasma. b) Discuss which collisional processes (α/e , α/D , or α/T) dominate each of these rates and why. c) How long will it take such a fusion-produced α particle to deposit half of its energy in the plasma? /+
- 2.30 The direction of energy transfer in Coulomb collisions of test particles with a background plasma depends on the test particle energy and other parameters. Estimate the particular test particle energies at which there is no energy exchange between test electrons, test protons and a Maxwellian background electron-proton plasma that has $T_e \neq T_i$, but T_e of the same order of magnitude as T_i . /+
- 2.31 Evaluate the ratio of energy diffusion to energy loss for electrons on the high energy tail ($m_e v^2/2 > T_e$) of a Maxwellian electron distribution function. Use this result to: a) find the probability that a tail electron will gain rather than lose energy; and b) discuss phenomenologically how the energy dependence of the Maxwellian tail of the electron distribution function is determined. //+
- 2.32 Consider a test electron with an energy of 10% of the electron temperature in a plasma. a) Show that the electron gains energy approximately linearly with time from a Maxwellian background of electrons. b) Estimate the time required (in terms of τ_e) for the test electron to acquire an energy approximately equal to the plasma electron temperature. //+
- 2.33 It is of interest to drive the current in a tokamak plasma by means other than via the usual inductive electric field. Thus, one often seeks [see N.J. Fisch, *Rev. Mod. Phys.* **59**, 175 (1987)] to drive currents by radiofrequency waves that impart momentum to a selected group of suprathermal ($v \gg v_{Te}$) electrons. Coulomb collision effects relax these suprathermal electrons back into the background distribution and thus limit the current produced. Estimate the steady-state “efficiency” J/P_d for such a process as follows. Consider a suprathermal electron that has a large velocity \mathbf{v}_0 relative to the thermal speed of background electrons which will be assumed to have a Maxwellian velocity distribution. Assume the ions in the plasma have charge Z_i , a Maxwellian distribution, and a comparable temperature to the background electrons. a) Show that the z -directed velocity component and speed of the suprathermal electron are governed by $dv_z/dt = -(2 + Z_i)\nu_0^{e/e}(v)v_z$ and $dv/dt = -\nu_0^{e/e}(v)v$, respectively. b) Combine these equations and show that for $v_{Te} < v < v_0$ their solution can be written as $v_z = v_{z0}[v(t)/v_0]^{2+Z_i}$. c) Then, show that the current induced in the plasma by one suprathermal electron over the time it takes for it to slow down to the thermal energy of the background electrons is

$$J_z = q_e \int dt v_z \simeq \frac{q_e v_{z0}}{\nu_0^{e/e}(v_0)} \frac{1}{5 + Z_i}.$$

d) However, show that the sum over an isotropic distribution of such suprathermal electrons yields no net current in the plasma. Next, consider the effect of a small momentum input via radiofrequency waves at $\mathbf{v}_0 = v_0 \hat{\mathbf{e}}_z$ that increases the electron velocity to $(v_0 + \delta v) \hat{\mathbf{e}}_z$ where $\delta v \ll v_0$. e) Calculate the ratio of the perturbed current δJ to the power (energy) input δP_d from the wave needed to produce this change and show it is given by

$$\frac{\delta J}{\delta P_d} = \frac{4}{5 + Z_i} \frac{q_e}{m_e \nu_0^{e/e}(v_0) v_0} \propto v_0^2.$$

f) Also consider wave momentum input in directions perpendicular to the initial suprathermal velocity direction z with $v_{z0} \neq 0$; show that it too can induce current in the z direction (with reduced efficiency) and explain physically how this is possible. g) Finally, show that when the current and power dissipated are normalized to $n_e q_e v_{Te}$ and $n_e m_e v_{Te}^2 \nu_0^{e/e}(v_{Te})$, respectively, the normalized steady-state “current-drive efficiency” for z -directed momentum input is given by

$$\frac{J}{P_d} = \frac{4}{5 + Z_i} \left(\frac{v_0}{v_{Te}} \right)^2.$$

h) In what range of speeds is this type of current drive most efficient? i) How does it compare to the normalized efficiency J/P_d for the usual ohmic current-drive by an electric field with $|\mathbf{E}| \ll E_D$? //+/

- 2.34 a) Show that for test electrons with energies much larger than the electron temperature in an electron-ion plasma with $T_i \sim T_e$ that $\nu_{\varepsilon}^e \simeq [2/(2 + Z_i)] \nu_{\varepsilon}^e$ and that the velocity friction and diffusion coefficients can be written to lowest order as

$$\begin{aligned} \frac{\langle \Delta \mathbf{v} \rangle^e}{\Delta t} &= -(2 + Z_i) \nu_0^{e/e} \mathbf{v}, \\ \frac{\langle \Delta \mathbf{v} \Delta \mathbf{v} \rangle^e}{\Delta t} &= \nu_0^{e/e} [(1 + Z_i)(v^2 \mathbf{I} - \mathbf{v} \mathbf{v}) + (v_{Te}^2/v^2) \mathbf{v} \mathbf{v}]. \end{aligned}$$

b) How large are the most significant terms that have been neglected for the beam electrons in Problem 2.12 /+

- 2.35 A hydrogen ice pellet is injected into a hot Maxwellian electron-proton plasma with $T_e = T_i = 2$ keV and $n_e = 5 \times 10^{19} \text{ m}^{-3}$. Assume the pellet doubles the plasma density. a) Neglecting the energy expended in the ionization processes (~ 30 – 100 eV), what is the temperature the hot plasma and the cold, pellet produced plasma (at say 10 eV) will equilibrate to? b) Estimate the time scales on which the electron and ion plasma components become Maxwellians at their new temperatures, and equilibrate to a common temperature. //+
- 2.36 It is usually difficult to measure directly the ion temperature of hydrogenic ions (protons, deuterons, tritons) in a hot plasma. However, it is often possible to determine the temperature of trace amounts of impurity ions in hot plasmas by measuring the Doppler broadening of the line radiation produced by the de-excitation of excited, highly ionized states of the impurity ions. Show that the impurity temperature is close to the ion temperature in Maxwellian plasmas with comparable electron (e), ion (i), and impurity (Z) temperatures as follows. Assume for simplicity that the impurities are heated only through Coulomb

collisions with the hot plasma electrons and the dominant, hydrogenic ions. a) First, write down an energy balance equation for the impurity species. b) Next, show that in equilibrium since the impurity mass is much closer to that of the hydrogenic ions than to that of the electrons, the impurity temperature can be written as

$$\begin{aligned} T_Z &\simeq T_i - \left(\bar{\nu}_e^{Z/e} / \bar{\nu}_e^{Z/i} \right) (T_i - T_e) \\ &= T_i - \left(\frac{n_e}{n_i Z_i^2} \right) \left(\frac{m_e}{m_i} \right)^{1/2} \left(\frac{T_i}{T_e} \right)^{3/2} (T_i - T_e). \end{aligned}$$

c) Finally, estimate the difference between the impurity and ion temperatures for $T_i = 10$ keV, $T_e = 5$ keV in a predominantly electron-deuteron plasma. //+

2.37 Using the formulas in Section 2.10, show that the total electron collision frequency ν_e for a multiple ion species, impure plasma is as implied in (2.44). /+

2.38 Using the formulas in Section 2.10, show that the impurity factor f_i given in (2.47) is correct. /+

2.39 Using the formulas in Section 2.10, show that the impurity factor f_{i-e} given in (2.49) is correct. /+

2.40 a) Show that for a fast ion of mass m_f and charge $Z_f e$ with $v_{Ti} \ll v_f \ll v_{Te}$ that is slowing down in a plasma composed of a mixture of ions of mass m_i and charge $Z_i e$ the slowing down is governed by (2.133), with the fast ion slowing down time τ_S unchanged, but that the critical speed v_c and energy ε_c are now given by

$$v_c^3 \equiv \frac{3\sqrt{\pi}}{4} \frac{m_e}{m_f} [Z]_m v_{Te}^3, \quad \varepsilon_c \simeq 15 T_e \left(\sqrt{\frac{m_f}{m_p}} [Z]_m \right)^{2/3}, \quad [Z]_m \equiv \sum_i \frac{n_i Z_i^2 / n_e}{(m_i / m_f)}.$$

Here, $[Z]_m$ is a mass-weighted effective Z_i for energy transfer processes in an impure plasma. b) For the parameters of Problem 2.29, what fraction of the alpha particle energy is transferred to the plasma ions and electrons? //+

2.41 Estimate the distance traveled by a fusion-produced 3.52 MeV α particle in slowing down in an infinite, homogeneous thermonuclear plasma as follows. a) First, calculate the alpha particle energy loss rate per unit distance traveled ($d\varepsilon/dz$) in terms of quantities derived in Section 2.11. b) Then, integrate to obtain the total distance z the alpha particle travels in slowing down from its initial velocity to the thermal velocity of the background plasma. c) Finally, estimate the distance traveled for the parameters of Problem 2.29 using the formulas developed in Problem 2.40. //+

2.42 Determine the current driven in a tokamak plasma by the fast ions introduced by energetic neutral beam injection [T. Ohkawa, *Nuclear Fusion* **10**, 185 (1970)] as follows. Consider introducing a beam of fast ions of density n_f , and charge $Z_f e$ with velocity \mathbf{V}_f such that $v_c \ll V_f \ll v_{Te}$. a) Calculate the relative flow $\mathbf{V}_e - \mathbf{V}_i$ induced by the beam ions for a plasma having ions of charge Z_i and density n_i . Assume $n_f \ll n_e$ and that the beam ions transfer their momentum only to plasma electrons for simplicity. b) Show that the net current in the plasma due to the three plasma components is given by $\mathbf{J} = n_f Z_f e \mathbf{V}_f (1 - Z_f / Z_i)$. c) Explain physically why there is no current when the fast beam ions have the same charge as the background ions, which is sometimes called a plasma

shielding effect. [Hint: The beam momentum input to the electrons is the same as the loss of fast ion momentum by collisions with the Maxwellian electron background, namely $m_f n_f \bar{v}_S^{f/e} \mathbf{V}_f$.] //+

- 2.43 For the case where there are no direct particle losses during fast ion slowing down ($\tau_{cx} \rightarrow \infty$), show that the fraction of fast ion energy transferred to the background plasma ions can be written as

$$G_i = \frac{2}{x^2} \left[-\frac{1}{6} \ln \frac{(1+x)^2}{1-x+x^2} + \frac{1}{\sqrt{3}} \arctan \frac{2x-1}{\sqrt{3}} + \frac{1}{\sqrt{3}} \arctan \frac{1}{\sqrt{3}} \right]$$

in which $x \equiv v_0/v_c$. //+

- 2.44 For the parameters of Problem 2.29, calculate the fast ion slowing down and energy transfer characteristics for a D-T fusion-produced alpha particle: a) the critical energy ε_c , and b) the total lifetime from birth to thermalization in the background D-T plasma. and c) the fraction of the alpha particle energy that will be transferred to the background plasma electrons and ions. /+
- 2.45 In the early, 1970s experiments that injected energetic neutral beams into tokamak plasmas there was concern that charge-exchange of the injected fast ions with neutrals in the plasma would cause the fast ions to be lost from the plasma before they could deposit their energy in the background electrons and ions. Consider 40 keV deuterium beam injection into a $n_e = 2 \times 10^{13} \text{ cm}^{-3}$, $T_e = 1.3 \text{ keV}$, $T_i = 0.5 \text{ keV}$ electron-deuteron plasma. a) What are the critical energy ε_c , slowing down time τ_S and fast ion lifetime τ_f for fast ions in this plasma? b) In the absence of charge-exchange losses, what fraction of the fast ion energy is transferred to the background plasma electrons, and ions? c) Assuming a charge-exchange cross section of $\sigma_{cx} = 7 \times 10^{-16} \text{ cm}^2$ and a neutral density of $n_n = 2 \times 10^8 \text{ cm}^{-3}$, what is τ_{cx} at the initial fast ion energy? (Since $\sigma_{cx} v$ is approximately constant below 20 keV per nucleon, τ_{cx} is nearly independent of energy.) d) How much does charge-exchange reduce the fractions of fast ion energy transferred to the background plasma electrons and ions? e) Which transfer fraction is affected the most? f) Why? /+
- 2.46 Energetic neutral atoms from neutral beams are absorbed in plasmas via the atomic collision processes of electron ionization, proton ionization and charge exchange. The ionization processes are $\sim \sigma_{ion}/(\sigma_{cx} + \sigma_{ion})$ probable ($\sim 30\%$ for the parameters of the preceding problem). They produce an electron whose initial speed is approximately the same as the injected fast neutral atom but whose kinetic energy is much lower. a) For the parameters of the preceding problem, what is the energy of such electrons? Since such electrons are born with low energies and take energy from the background plasma as they are heated to the plasma electron temperature, they represent an initial heat sink. b) Approximately how long does it take for these electrons to be heated by the plasma to the background electron temperature of 1.3 keV? (Hint: See Problem 2.32.) c) How does this time compare to the fast ion slowing down time τ_S ? d) About how long does it take for the injected energetic neutral beam to add net energy to the plasma? //+
- 2.47 In the “wet wood burner” approach to controlled thermonuclear fusion [J.M. Dawson, H.P. Furth and F.H. Tenney, *Phys. Rev. Lett.* **26**, 1156 (1971)] it is proposed to obtain energy multiplication through fusion reactions of energetic deuterons as they slow down in a background triton plasma. a) Show that the

energy multiplication factor F , which is defined as the ratio of fusion energy produced to the initial deuteron energy ε_0 , can be written as

$$F = \left(\frac{\varepsilon_f}{\varepsilon_0} \right) (n\tau_S) \int_0^{v_0} \frac{v^3 dv}{v^3 + v_c^3} \sigma_f(v) \equiv \left(\frac{\varepsilon_f}{\varepsilon_0} \right) (n\tau_S) \overline{\sigma_f v}$$

in which ε_f is the energy produced per fusion and $\sigma_f(v)$ is the speed- (energy-) dependent fusion cross section. b) For D-T fusion with $\varepsilon_f = 22.4$ MeV (17.6 MeV from the reaction products and 4.8 MeV from assuming energy multiplication by neutrons absorbed in a surrounding lithium blanket) and $\overline{\sigma_f v} \simeq 2.8 \times 10^{-22} \text{ m}^3/\text{s}$ for 120 keV deuterons, find the minimum electron temperature at which energy multiplication is possible. c) For this “critical” temperature, what is the probability that a deuteron will undergo a fusion reaction during its slowing down? //+

- 2.48 Consider the angular or perpendicular diffusion of a fast proton with energy 40 keV injected into a Maxwellian electron-proton plasma that has $T_e = T_i = 1$ keV and $n_e = 3 \times 10^{19} \text{ m}^{-3}$. a) Estimate the time at which Coulomb collisions scatter the velocity space angle of the fast proton through $\delta\vartheta = \delta v_\perp/v = 0.1$ radian ($\sim 6^\circ$). b) Compare this time to the fast ion slowing down time τ_S defined in (2.130). c) Discuss the physical reason why one of these times is much shorter than the other. //+
- 2.49 Consider the proposition that an electric field \mathbf{E} is applied to keep fast ions with $v_{Ti} \ll v \ll v_{Te}$ from slowing down in a plasma. a) First, calculate the momentum loss rate of the fast ion and find its minimum as a function of the fast ion speed v . b) Next, calculate the minimum electric field [in terms of the Dreicer field defined in (2.28)] required to prevent fast ions from slowing down. c) Then, discuss the degree to which such an electric field would cause runaway electrons. d) Estimate the rates of perpendicular and parallel diffusion at the fast ion speed at which the minimum momentum loss rate occurs. e) Finally, discuss the effects these processes might have on the proposed scheme (cf., Fig. 2.7). //+
- 2.50 a) Show that for a fast ion slowing down in the plasma described in Problem 2.40 the dynamical friction and diffusion coefficients can be written to lowest order as

$$\begin{aligned} \frac{\langle \Delta \mathbf{v} \rangle^f}{\Delta t} &= - \left([Z]_m + (Z_{\text{eff}} + [Z]_m) \frac{v_c^3}{v^3} \right) \frac{\mathbf{v}}{\tau_S} \\ \frac{\langle \Delta \mathbf{v} \Delta \mathbf{v} \rangle^f}{\Delta t} &= \frac{1}{\tau_S} \left(Z_{\text{eff}} \frac{v_c^3}{v^3} (v^2 \mathbf{I} - \mathbf{v} \mathbf{v}) + \frac{2[T_e + T_{\text{eff}}(v_c^3/v^3)]}{m_f} \frac{\mathbf{v} \mathbf{v}}{v^2} \right) \end{aligned}$$

in which the angular scattering Z_{eff} is defined in (2.43), the energy transfer or mass-weighted $[Z]_m$ is defined in Problem 2.40 and the effective ion temperature is defined by

$$T_{\text{eff}} \equiv \frac{1}{[Z]_m} \sum_i \frac{n_i Z_i^2 / n_e}{(m_i / m_f)} T_i.$$

- b) How large is the most significant term that has been neglected in these approximate results and where does it contribute for fast ions slowing down for the situation described in Problem 2.48? //+

- 2.51 Write a Monte Carlo type computer code for exploring the Coulomb scattering of energetic test electrons in an electron-proton plasma. Use it to determine numerically the answers to parts a) and b) of Problem 2.12. //+
- 2.52 Write a Monte Carlo type computer code for exploring the Coulomb collision processes for fast ions slowing down in an electron-ion plasma. Use it to determine numerically the answers to the questions in Problem 2.48. ///+